Viscous fingering in electro-osmotic flows

John Lowengrub

Departments of Mathematics and Biomedical Engineering

University of California, Irvine

IPAM Workshop 1, Sept 17, 2025.

Acknowledgements

- Pedro H.A. Anjos (U. Federal de Pernambuco)

- Meng Zhao (Huazhong U. Sci. Tech

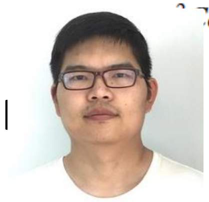

- Wenjun Ying (Shanghai Jiao Tong U.)

- Shuwang Li (Ill. Inst. Techn.)

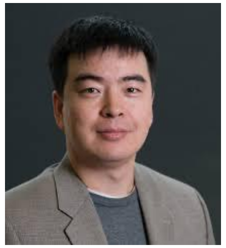

PHYSICAL REVIEW FLUIDS **7**, 053903 (2022)

Electrically controlled self-similar evolution of viscous fingering patterns

Pedro H. A. Anjos,[1,*,†] Meng Zhao,[2,*,‡] John Lowengrub,[3,§] and Shuwang Li[1,‖]
[1] *Department of Applied Mathematics, Illinois Institute of Technology, Chicago, Illinois 60616, USA*
[2] *Center for Mathematical Sciences, Huazhong University of Science and Technology, Wuhan 430074, China*
[3] *Department of Mathematics, University of California at Irvine, Irvine, California 92697, USA*

Commun. Comput. Phys.
doi: 10.4208/cicp.OA-2022-0128

Vol. 33, No. 2, pp. 399-424
February 2023

Numerical Study on Viscous Fingering Using Electric Fields in a Hele-Shaw Cell

Meng Zhao[1,*], Pedro Anjos[2], John Lowengrub[3], Wenjun Ying[4] and Shuwang Li[2]

[1] *Center for Mathematical Sciences, Huazhong University of Science and Technology, Wuhan, Hubei 430074, China.*
[2] *Department of Applied Mathematics, Illinois Institute of Technology, Chicago, IL 60616, USA.*
[3] *Department of Mathematics, University of California Irvine, Irvine, CA 92697, USA.*
[4] *School of Mathematical Sciences, MOE-LSC and Institute of Natural Sciences, Shanghai Jiao Tong University, Shanghai 200240, China.*

Outline of talk

- Introduction to interface problems and viscous fingering
- Viscous fingering with electro-osmotic flows
- Linear stability analysis
- Nonlinear simulations
- Summary and future work

Introduction: Pattern forming systems

Bacterial colonies

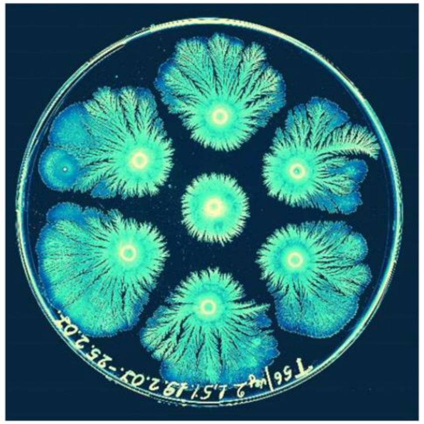

Solidification

Flame propagation

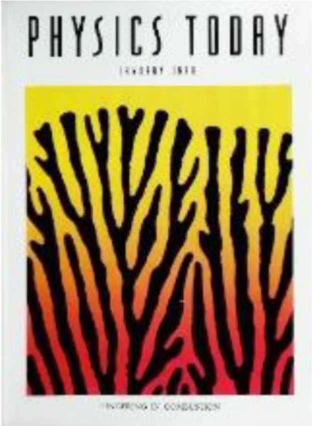

- Long time pattern formed by multiple ramification events and finger competition.
- The most important system information is contained at the interface.
- The complexity of this system is remarkable given its physical simplicity.
- Viscous fingering is possibly the simplest system among a family of pattern forming systems that exhibit interfacial instabilities.

Hele-Shaw problem

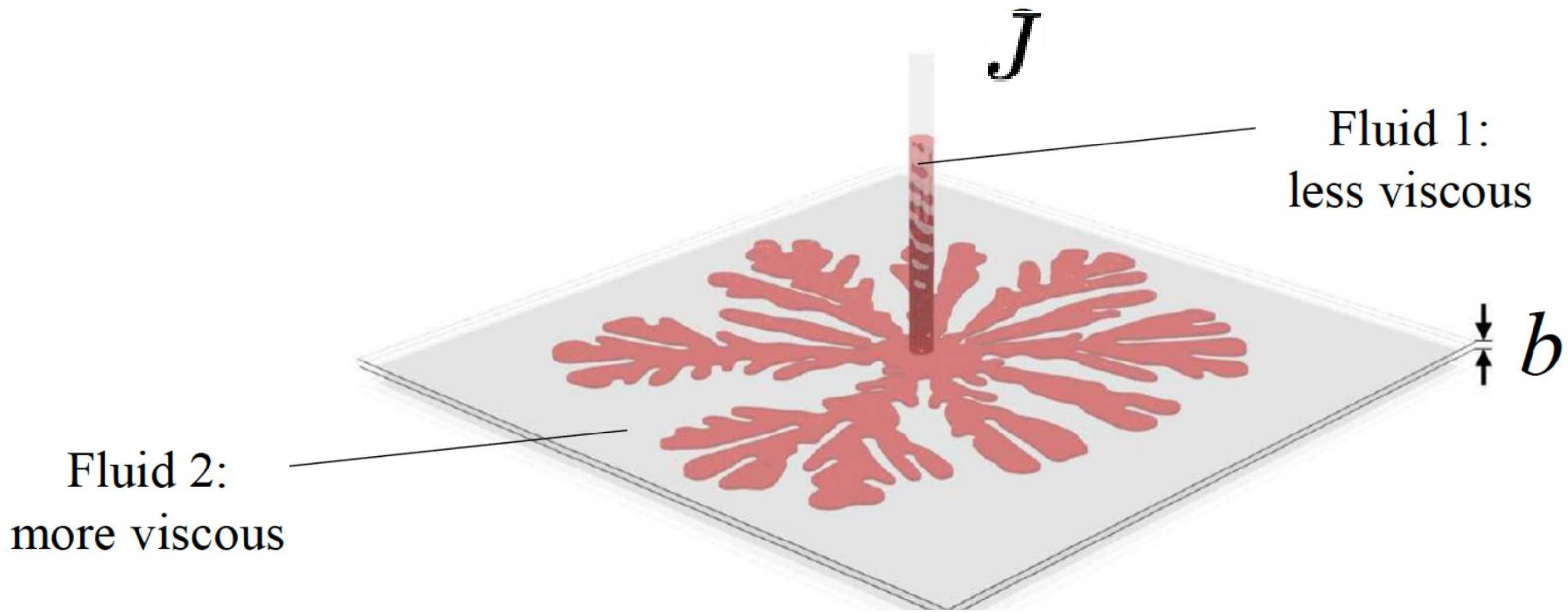

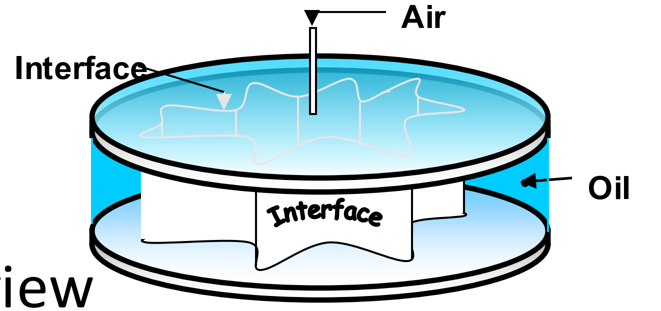

side view

- Hele-Shaw problem is a classical example for studying the interface dynamics.
- One fluid displaces an existing fluid between two parallel plate with a small gap.
  Application: oil recovery in petroleum engineering, natural gas storage
- Saffman-Taylor instability (fingering pattern) only occurs when less viscous fluid is injected into existing more viscous fluid.

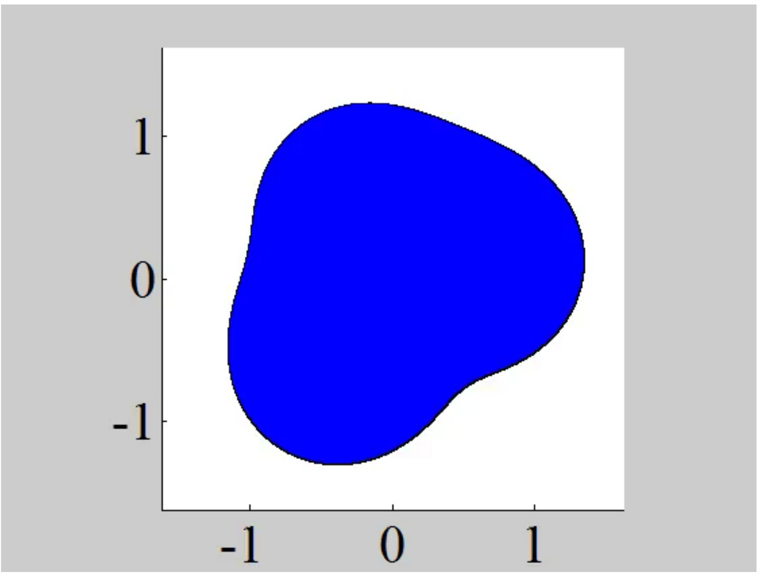

Zhao et al., Commun. Comp. Phys. (2017)

Mathematical model

Darcy Flow (exterior problem, incompressible fluid):

$$\mathbf{u} = -M\nabla P, \quad \mathbf{x} \in E_2$$

Hydraulic mobility

$$M = \frac{b^2}{12\eta}$$

$$\nabla \cdot \mathbf{u} = 0, \quad \mathbf{x} \in E_2$$

Incompressibility

$$[P]_t = \tau\kappa, \quad \mathbf{x} \in \Gamma(t)$$

Surface tension

$$\int_{\Sigma_0} \frac{\partial P}{\partial \mathbf{n}} ds = J(t)$$

Injection flux

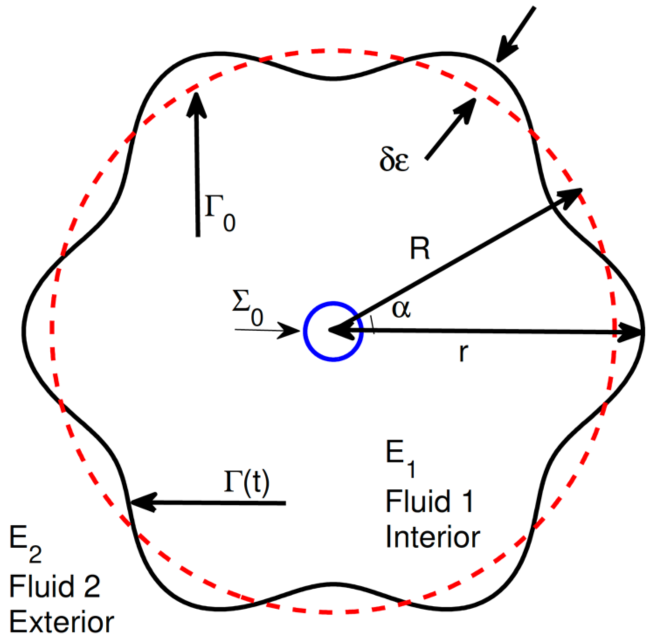

Interface dynamics: $\frac{d\mathbf{x}}{dt} = V\mathbf{n} + T\mathbf{s}.$

Normal velocity: $V = \mathbf{u} \cdot \mathbf{n}$

Tangential velocity: T

What drives the instability?

Growth morphologies are determined by the interaction of macroscopic driving forces and microscopic interfacial properties

- Macroscopic driving force: destabilizing effects, favors complex structures
  - ➢ Flow rate (injection flux J). Time scale: $t_J \sim R_0^2/J$

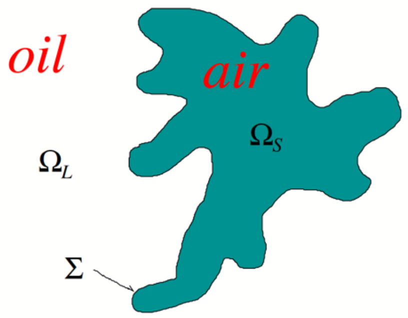

- Microscopic interfacial properties: stabilizing effects, favors compact structures structures
  - ➢ Surface tension τ Time scale: $t_\tau \sim R_0^3/(\tau M), \quad M = \dfrac{b^2}{12\eta}$

- Unbalanced time scale: $\dfrac{t_J}{t_\tau} \sim \dfrac{\tau M}{R_0 J}$

➢ Surface tension acts on longer time scales than flux as size grows. Saffman-Taylor Instability (J constant)

How to modify, or control, the instability?

- Modify the geometry

  - Time-dependent gap width (Zheng et al. 2015; Vaquero-Stainer et al. 2019,…)
  - Tapered walls (Al-Housseiny & Stone, 2013; Bongrand & Tsai, 2018; …)
  - Hele-Shaw cells with elastic walls (Pihler et al, 2018)

- Time-varying fluxes

  Cardoso & Woods (1995), Li et al. (2009), Fontana et al. (2014), Beeson-Jones & Woods (2017),….

  - Balanced time scale: $J = \bar{J}/R_0$

$$\frac{t_J}{t_\tau} \sim \frac{\tau M}{R_0 J} \sim \frac{\tau M}{\bar{J}}$$

- Surface tension acts on same time scale as flux, which decreases as system grows.

Time varying flux: Linear stability analysis

Perturbation: $r_\Sigma(\theta,t) = R(t) + \delta(t)\cos(k\theta)$

Growth: $J = R\dot{R} + O(\delta / R)^2$

Pressure:

(Control pressure)

$$J(t) = \frac{-P(t) + \tau / R}{Log(R_\infty) - Log(R)} + O(\delta / R)^2$$

Roughly linear reln between P and J

Shape evolution: $\boxed{(\delta / R)^{-1} (\delta / R)^{\bullet} = \frac{(k-2)}{R^2}(J - J_k)}$

Critical flux: $J_k = \frac{C_k}{R(t)}, \; C_k = \frac{k(k^2-1)}{k-2}$ Mode k fastest growing: $J_k{}^* = \frac{3k^2-1}{R(t)}$

$J > J_k$ unstable evolution (Saffman-Taylor)

$J = J_k$ self-similar evolution $\boxed{(\delta / R) = const.}$

$J < J_k$ perturbation decays stable evolution

Time varying flux: Nonlinear results

$$J = 84/R(t)$$

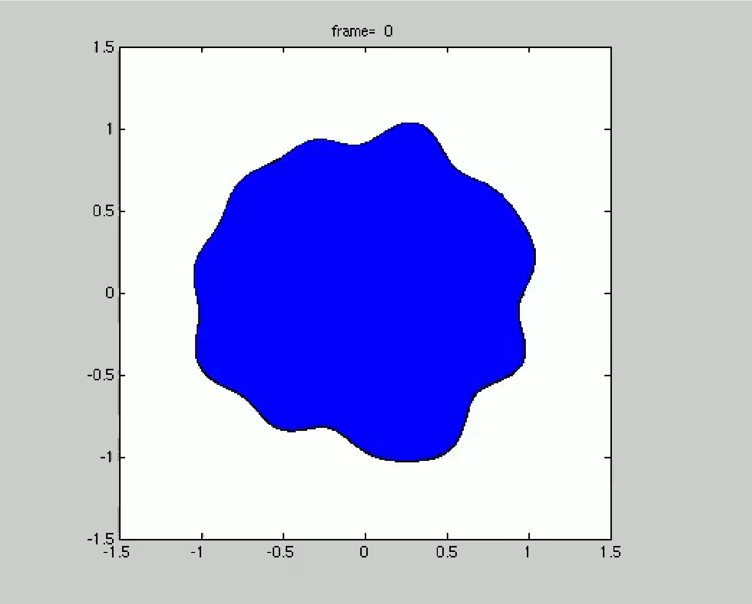

- Evolution to a 6-fold limiting shape, independent of IC.

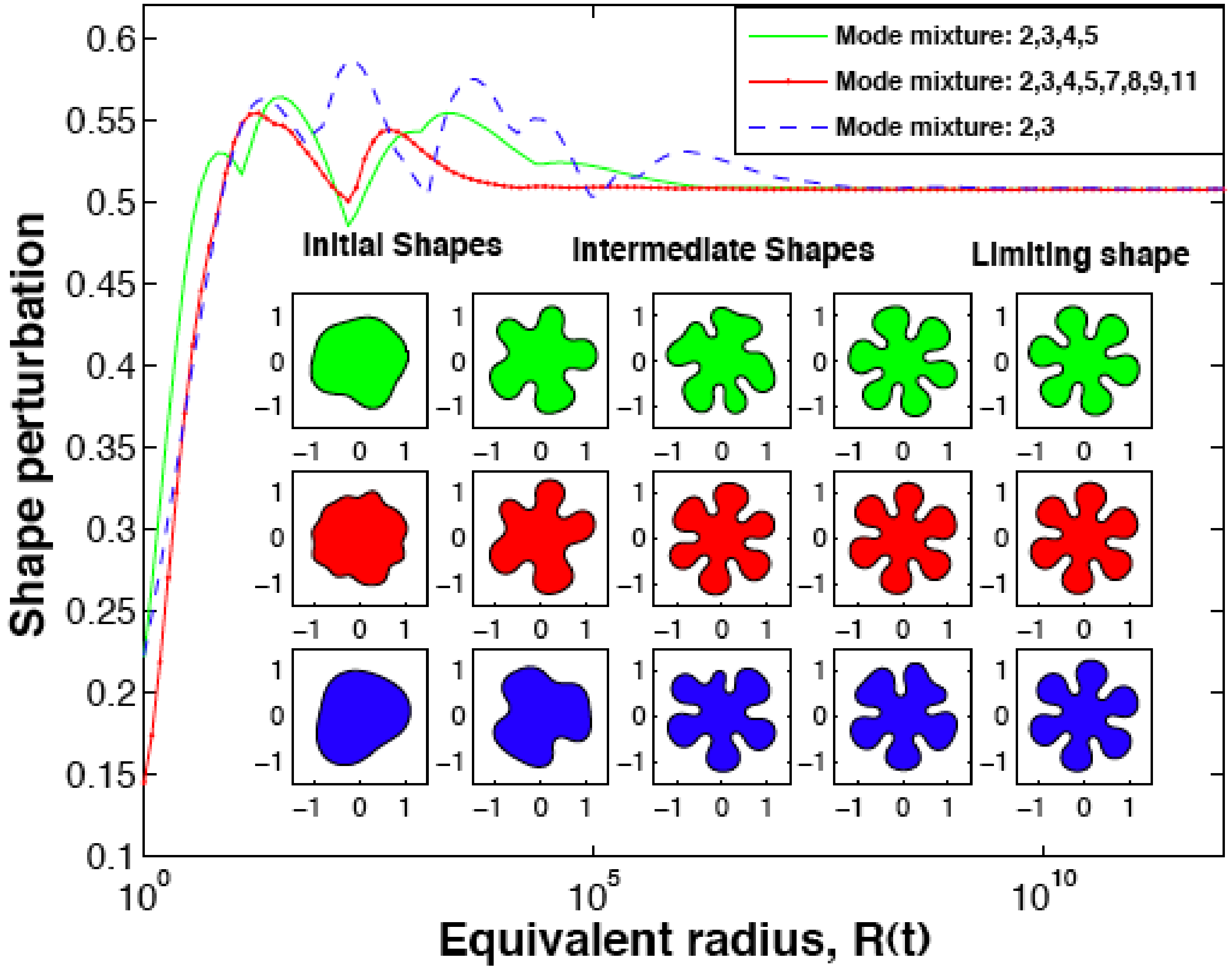

Spectrally accurate, rescaled boundary integral methods. Li & L. et al. (2007, 2009, 2017)

Time varying flux: Morphology diagram

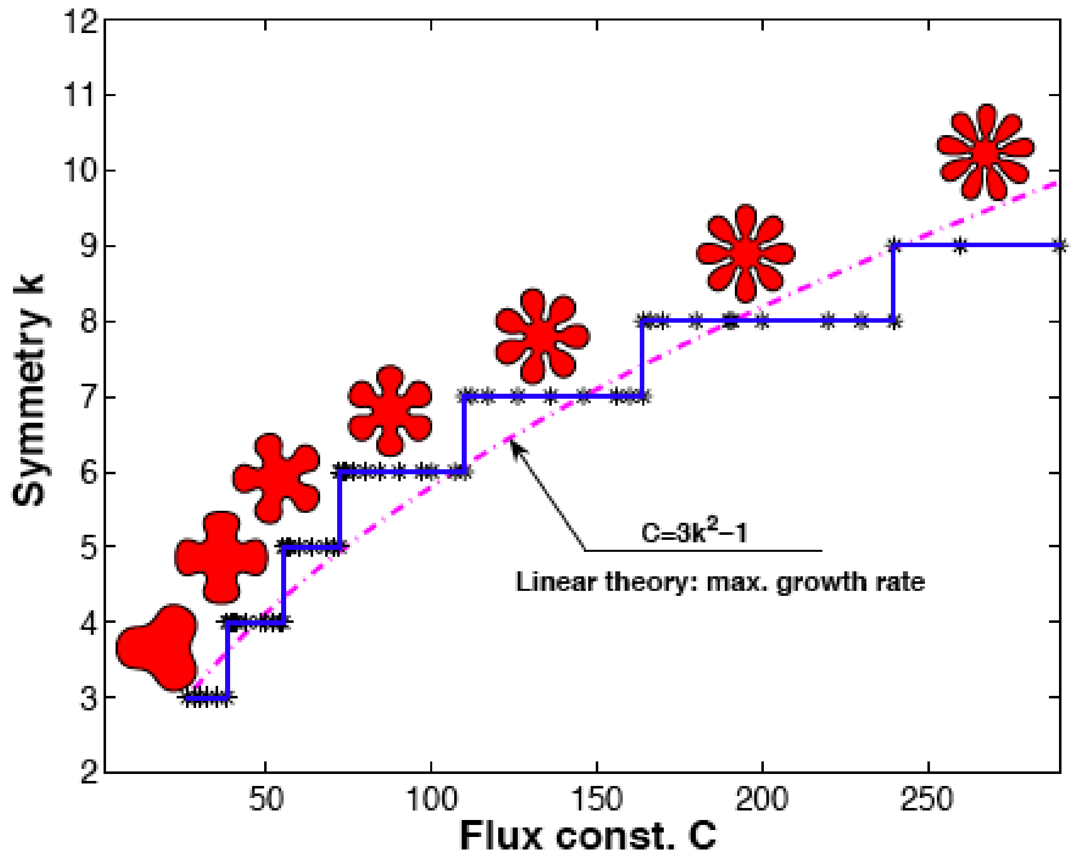

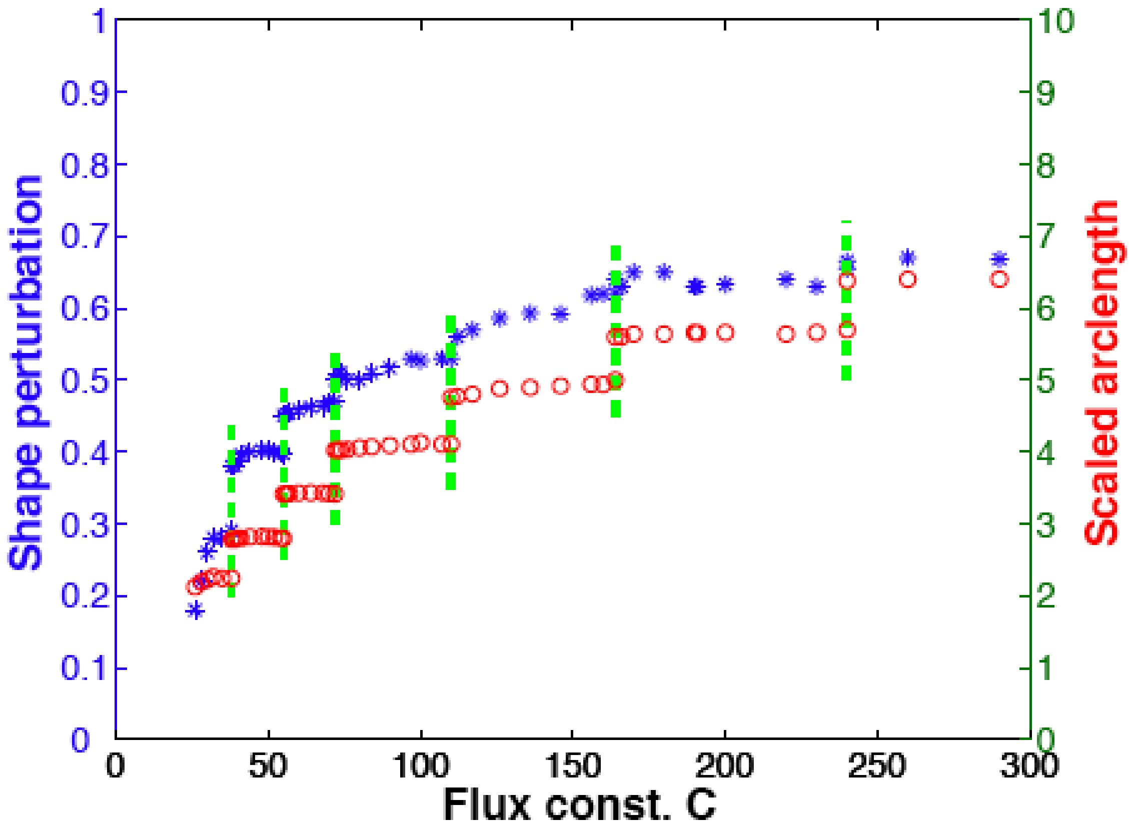

- Sharp transitions between solution families
- Perturbations grow as C increases. Singular limiting shape for C large? (thinning necks)

Time varying flux: Experimental validation I

Liquid Crystal Institute, KSU

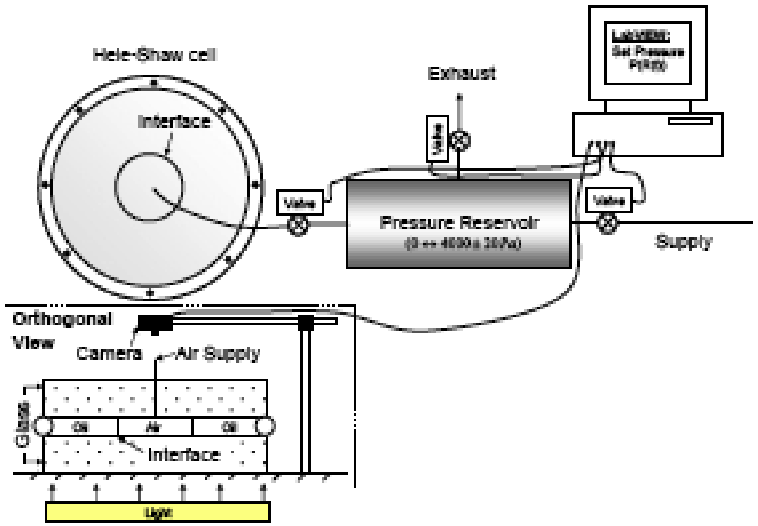

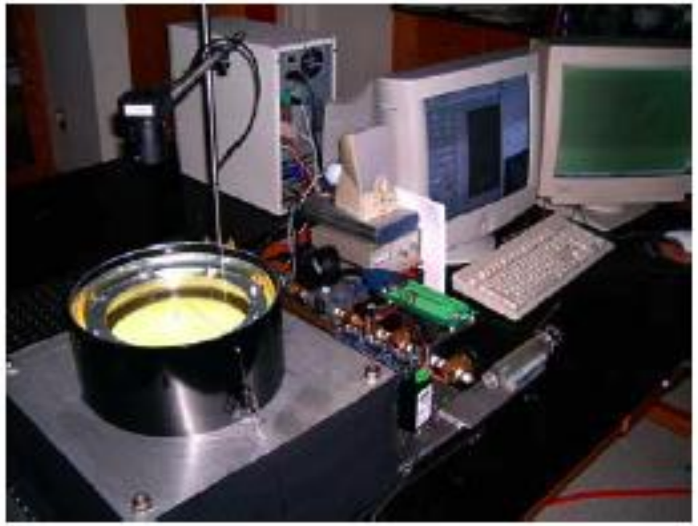

Theory

Experiments

Applied flux $J(t) = \dfrac{C}{R(t)}$

No feedback needed $R(t)^3 - R(0)^3 = 3Ct$

$$P(t) = J(t)\log\frac{R_\infty}{R(t)} + \frac{1}{R(t)}$$

- Li et al. (2009)

Time varying flux: Experimental validation II

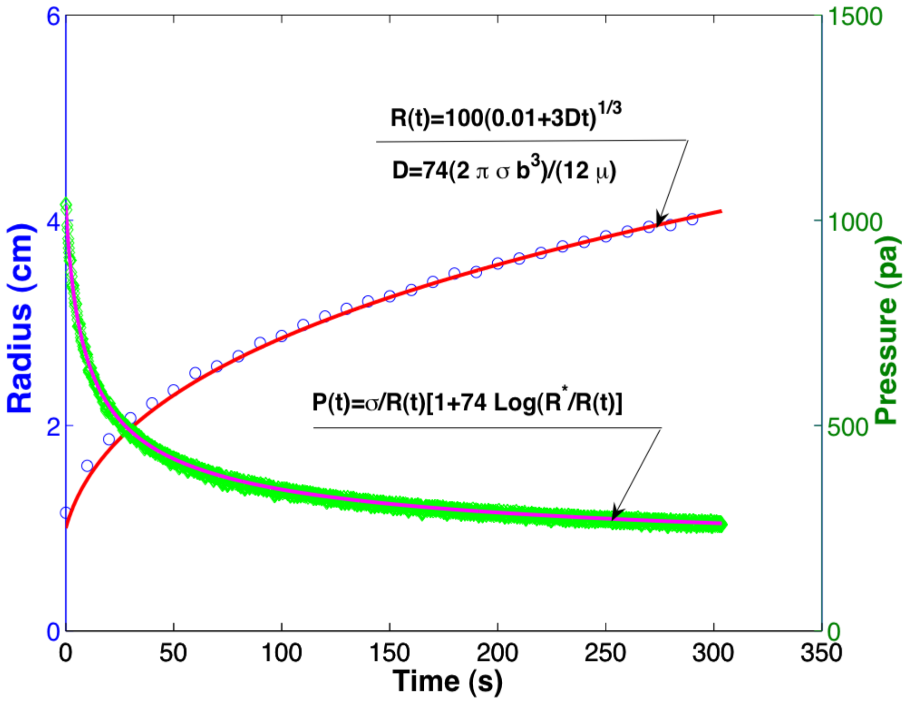

Experimental demonstration that the symmetry of an expanding bubble in castor oil

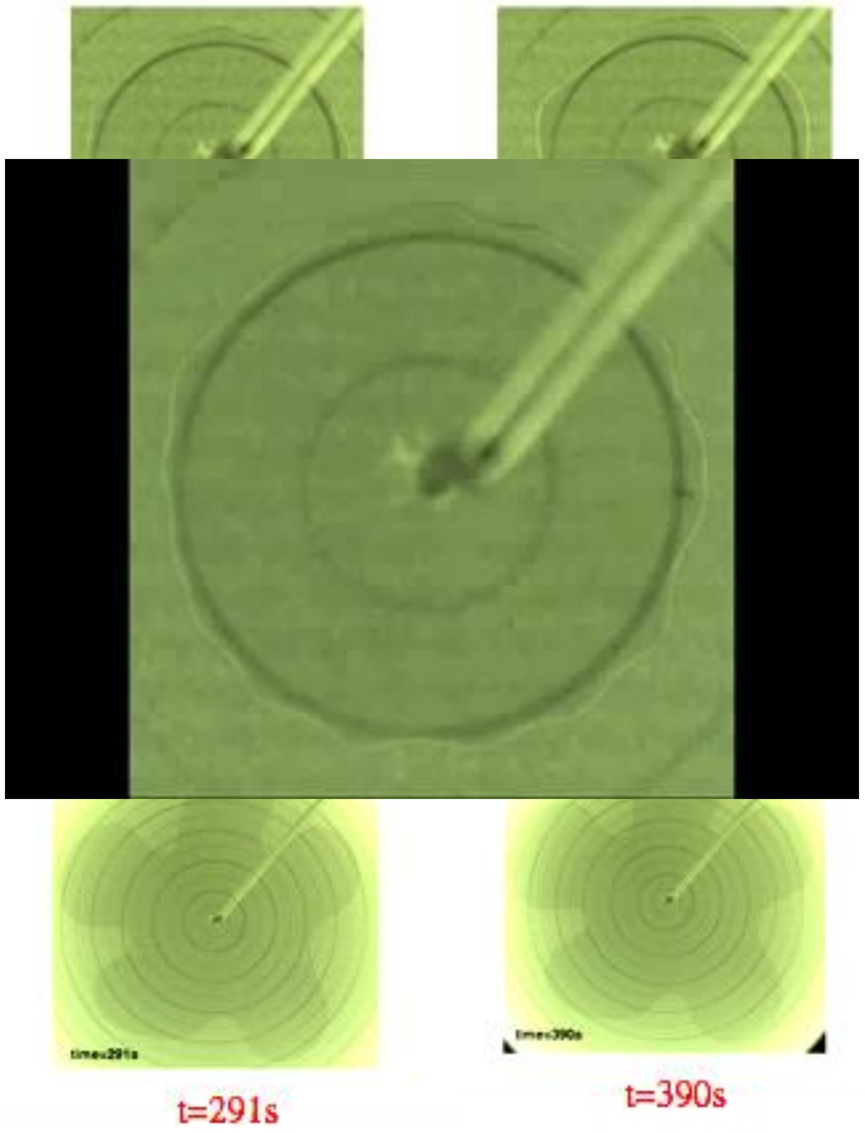

- C=74 theory predicts a 5-fold shape

Time varying flux: Experimental validation III

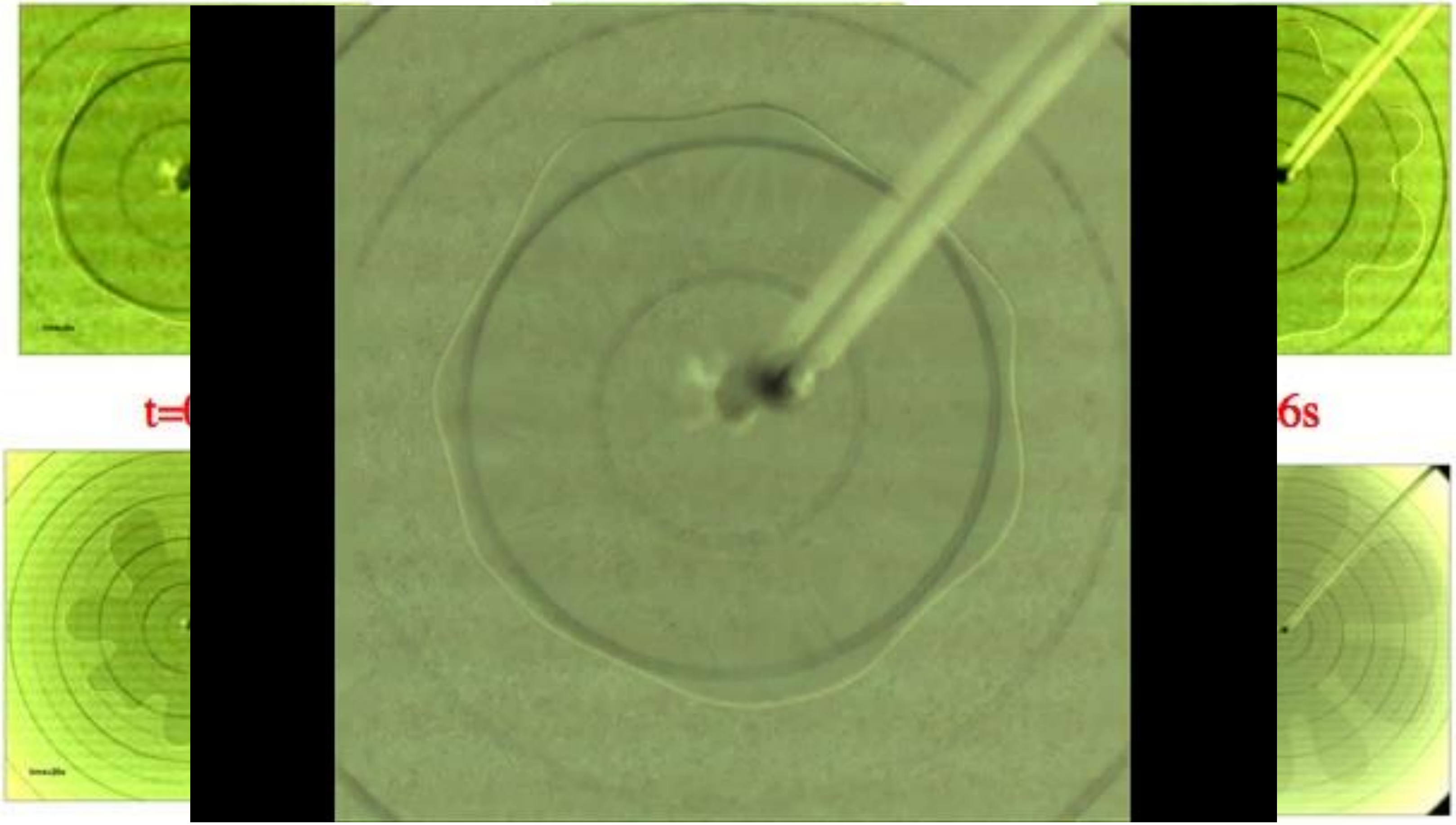

t=20s t=40s t=140s

- C=191 theory predicts a 8-fold shape
- Have to get to larger sizes as C increases to see limiting shapes. Evolution is faster.

External fields can also modify the instability

PRL **119,** 174501 (2017) PHYSICAL REVIEW LETTERS week ending 27 OCTOBER 2017

Electrokinetic Control of Viscous Fingering

Mohammad Mirzadeh[1] and Martin Z. Bazant[1,2,*]

[1]*Department of Chemical Engineering, Massachusetts Institute of Technology, Cambridge, Massachusetts 02139, USA*

[2]*Department of Mathematics, Massachusetts Institute of Technology, Cambridge, Massachusetts 02139, USA*

(Received 19 June 2017; published 26 October 2017)

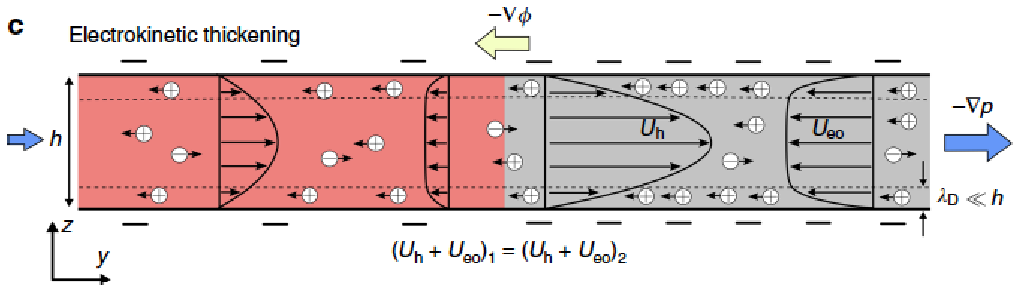

- Electro-osmotic flows can resist pressure driven flows, leading to an apparent increase in viscosity (stabilization)

Electric double layer (EDL) at glass surface. Glass is negatively charged due to dissociation of ionic surface groups. Excess counter ions accumulate near glass. External electric field drives electro-osmotic flow in addition to pressure driven flow. Can enhance or suppress instability.

ARTICLE

https://doi.org/10.1038/s41467-019-11939-7 OPEN

Active control of viscous fingering using electric fields

Tao Gao[1,4], Mohammad Mirzadeh[1,4], Peng Bai[1,3], Kameron M. Conforti[1] & Martin Z. Bazant[1,2]

NATURE COMMUNICATIONS | (2019)10:4002 | https://doi.org/10.1038/s41467-019-11939-7 | www.nature.com/naturecomm

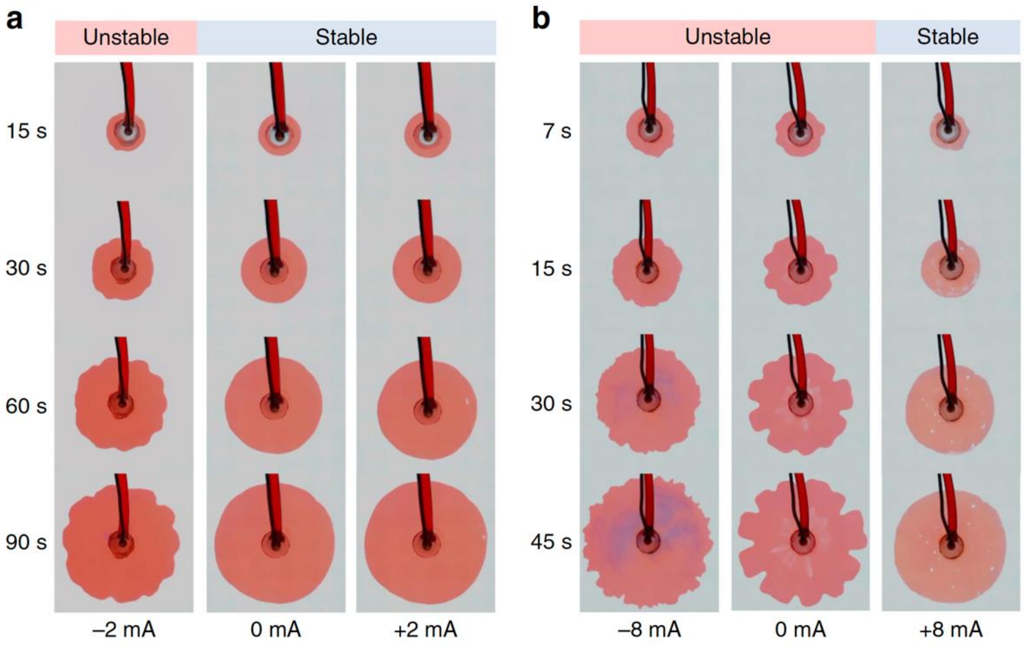

Mathematical model of viscous fingering with electro-osmotic flows

Darcy flow

Electro-osmotic flow (electric potential ϕ, k_{eo} electro-osmotic mobility)

$$\mathbf{u}_h = -k_h \nabla P, \mathbf{u}_{eo} = -k_{eo} \nabla \phi, \qquad \mathbf{x} \in \Omega$$

$$\mathbf{u} = \mathbf{u}_h + \mathbf{u}_{eo}, \qquad \mathbf{x} \in \Omega$$

Streaming current

E-O=-O current

$$\mathbf{i}_{sc} = -k_{eo} \nabla P, \mathbf{i}_e = -k_e \nabla \phi, \qquad \mathbf{x} \in \Omega$$

$$\mathbf{i} = \mathbf{i}_{sc} + \mathbf{i}_e, \qquad \mathbf{x} \in \Omega$$

incompressibility

No charge in liquid

$$\nabla \cdot \mathbf{u} = 0, \nabla \cdot \mathbf{i} = 0, \qquad \mathbf{x} \in \Omega$$

Interface conditions $[P]_t = \tau\kappa, [\phi] = 0, \qquad \mathbf{x} \in \Gamma(t)$

Injection flux

$$\int_{\Gamma_0} \mathbf{u} \cdot \mathbf{n} ds = 2\pi J,$$

Applied current

$$\int_{\Gamma_0} \mathbf{i} \cdot \mathbf{n} ds = 2\pi I.$$

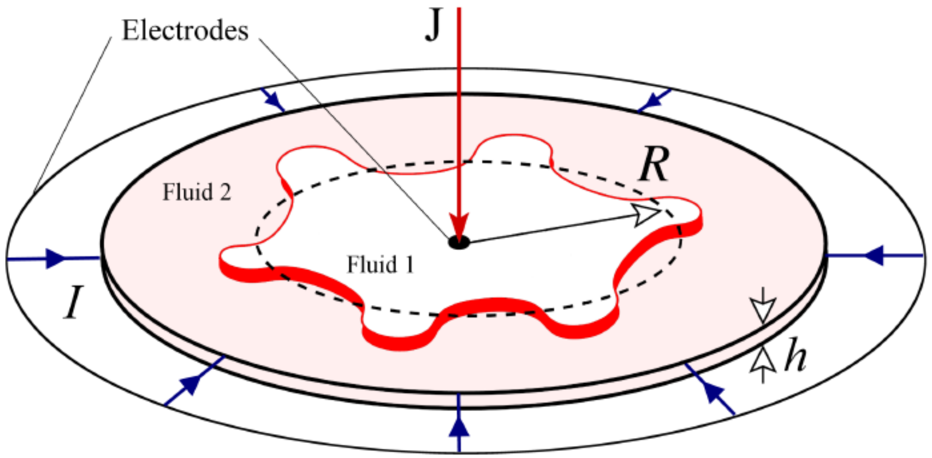

Interface dynamics:

$$\frac{d\mathbf{x}}{dt} = V\mathbf{n} + T\mathbf{s}.$$

Debye length $\lambda_D \sim 10 \text{ nm} \ll b$

$$K_j = -\varepsilon_j \zeta_j / \eta_j$$

Linear stability analysis I

- Perturbation: $r(\tilde{\alpha}, t) = R(t) + \epsilon\delta(t)\cos(n\tilde{\alpha}).$
- Shape evolution:

$$\left(\frac{\delta}{R}\right)^{-1}\frac{d}{dt}\left(\frac{\delta}{R}\right) = \frac{(k_{eo_2}k_{h_1} - k_{eo_1}k_{h_2})}{(k_{eo_1}+k_{eo_2})^2 - (k_{e_1}+k_{e_2})(k_{h_1}+k_{h_2})}\frac{2nI}{R^2}$$
$$+ \left(n\frac{k_{eo_1}^2 - k_{eo_2}^2 - (k_{e_1}+k_{e_2})(k_{h_1}-k_{h_2})}{(k_{eo_1}+k_{eo_2})^2 - (k_{e_1}+k_{e_2})(k_{h_1}+k_{h_2})} - 2\right)\frac{J}{R^2}$$
$$- \frac{\tau n(n^2-1)}{R^3}\frac{(k_{eo_2}^2 k_{h_1} + (k_{eo_1}^2 - (k_{e_1}+k_{e_2})k_{h_1})k_{h_2})}{(k_{eo_1}+k_{eo_2})^2 - (k_{e_1}+k_{e_2})(k_{h_1}+k_{h_2})}.$$

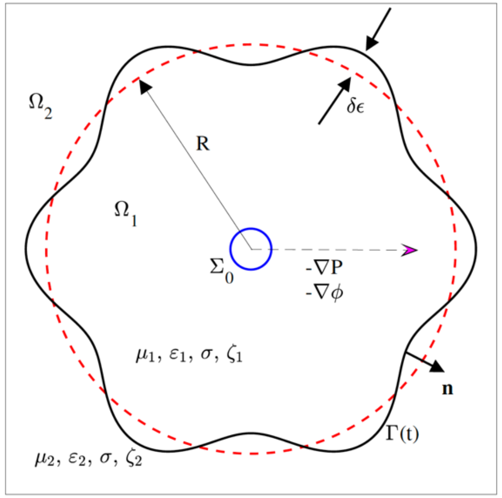

- The fastest growing mode

$$n_{max} = \sqrt{\frac{R}{3}\left(\frac{(2I(k_{eo_2}k_{h_1} - k_{eo_1}k_{h_2}) + J[k_{eo_1}^2 - k_{eo_2}^2 - (k_{e_1}+k_{e_2})(k_{h_1}-k_{h_2})])}{\tau[k_{eo_2}^2 k_{h_1} + (k_{eo_1}^2 - (k_{e_1}+k_{e_2})k_{h_1})k_{h_2}]} + \frac{1}{R}\right)}.$$

Linear stability analysis II

- Shape preserving current:

$$I_c = \Big(-[k_{eo_1}^2 - k_{eo_2}^2 - (k_{e_1} + k_{e_2})(k_{h_1} - k_{h_2})]J + \frac{\tau\mathcal{C}}{R}[k_{eo_2}^2 k_{h_1} + (k_{eo_1}^2 - (k_{e_1} + k_{e_2})k_{h_1})k_{h_2}]\Big)/2/(k_{eo_2}k_{h_1} - k_{eo_1}k_{h_2}),$$

  where $\mathcal{C}$ is a constant. When $\mathcal{C} = 3n_{max}^2 - 1$. The fastest growth mode unchanged.

- The fastest growing rate:

$$(\frac{\delta}{R})^{-1}\frac{d}{dt}(\frac{\delta}{R}) = \frac{2n_{max}^3\tau}{R^3}\frac{[k_{eo_2}^2 k_{h_1} + (k_{eo_1}^2 - (k_{e_1} + k_{e_2})k_{h_1})k_{h_2}]}{(k_{eo_1} + k_{eo_2})^2 - (k_{e_1} + k_{e_2})(k_{h_1} + k_{h_2})} - \frac{2J}{R^2}.$$

- J is a positive constant, the growth rate eventually is negatvie.
- J is zero, $R(t)$ remains unchanged.
- Critical flux

$$J_{crit} = \frac{n_{max}^3\tau}{R}\frac{[k_{eo_2}^2 k_{h_1} + (k_{eo_1}^2 - (k_{e_1} + k_{e_2})k_{h_1})k_{h_2}]}{(k_{eo_1} + k_{eo_2})^2 - (k_{e_1} + k_{e_2})(k_{h_1} + k_{h_2})}.$$

Nonlinear numerical solutions: Boundary integral method

- Take $\varphi_v = k_h P + k_{eo}\phi$ and $\varphi_c = k_{eo} P + k_e \phi$.
- Use potential theory

$$
\begin{aligned}
\varphi_v &= \frac{1}{2\pi}\int_{\Gamma(t)} \gamma_1(\mathbf{y}) \frac{\partial \ln|\mathbf{x}-\mathbf{y}|}{\partial \mathbf{n}(\mathbf{y})} ds(\mathbf{y}) + J \ln|\mathbf{x}|, \\
\varphi_c &= \frac{1}{2\pi}\int_{\Gamma(t)} \gamma_2(\mathbf{y}) \frac{\partial \ln|\mathbf{x}-\mathbf{y}|}{\partial \mathbf{n}(\mathbf{y})} ds(\mathbf{y}) + I \ln|\mathbf{x}|,
\end{aligned}
$$

- Use boundary conditions

$$
\begin{aligned}
&\left(\frac{k_{e_1}}{k_{h_1}k_{e_1}-k_{eo_1}^2}+\frac{k_{e_2}}{k_{h_2}k_{e_2}-k_{eo_2}^2}\right)\gamma_1+\frac{1}{\pi}\left(\frac{k_{e_1}}{k_{h_1}k_{e_1}-k_{eo_1}^2}-\frac{k_{e_2}}{k_{h_2}k_{e_2}-k_{eo_2}^2}\right)\int_{\Gamma(t)}\gamma_1(\mathbf{y})\frac{\partial \ln|\mathbf{x}-\mathbf{y}|}{\partial \mathbf{n}(\mathbf{y})}ds(\mathbf{y}) \\
&-\left(\frac{k_{eo_1}}{k_{h_1}k_{e_1}-k_{eo_1}^2}+\frac{k_{eo_2}}{k_{h_2}k_{e_2}-k_{eo_2}^2}\right)\gamma_2-\frac{1}{\pi}\left(\frac{k_{eo_1}}{k_{h_1}k_{e_1}-k_{eo_1}^2}-\frac{k_{eo_2}}{k_{h_2}k_{e_2}-k_{eo_2}^2}\right)\int_{\Gamma(t)}\gamma_2(\mathbf{y})\frac{\partial \ln|\mathbf{x}-\mathbf{y}|}{\partial \mathbf{n}(\mathbf{y})}ds(\mathbf{y}) \\
&= 2\tau\kappa-\left(\frac{k_{e_1}}{k_{h_1}k_{e_1}-k_{eo_1}^2}-\frac{k_{e_2}}{k_{h_2}k_{e_2}-k_{eo_2}^2}\right)J\ln|\mathbf{x}|^2+\left(\frac{k_{eo_1}}{k_{h_1}k_{e_1}-k_{eo_1}^2}-\frac{k_{eo_2}}{k_{h_2}k_{e_2}-k_{eo_2}^2}\right)I\ln|\mathbf{x}|^2,
\end{aligned}
$$

$$
\begin{aligned}
&-\left(\frac{k_{eo_1}}{k_{h_1}k_{e_1}-k_{eo_1}^2}+\frac{k_{eo_2}}{k_{h_2}k_{e_2}-k_{eo_2}^2}\right)\gamma_1-\frac{1}{\pi}\left(\frac{k_{eo_1}}{k_{h_1}k_{eo_1}-k_{eo_1}^2}-\frac{k_{eo_2}}{k_{h_2}k_{e_2}-k_{eo_2}^2}\right)\int_{\Gamma(t)}\gamma_1(\mathbf{y})\frac{\partial \ln|\mathbf{x}-\mathbf{y}|}{\partial \mathbf{n}(\mathbf{y})}ds(\mathbf{y}) \\
&+\left(\frac{k_{h_1}}{k_{h_1}k_{e_1}-k_{eo_1}^2}+\frac{k_{h_2}}{k_{h_2}k_{e_2}-k_{eo_2}^2}\right)\gamma_2+\frac{1}{\pi}\left(\frac{k_{h_1}}{k_{h_1}k_{e_1}-k_{eo_1}^2}-\frac{k_{h_2}}{k_{h_2}k_{e_2}-k_{eo_2}^2}\right)\int_{\Gamma(t)}\gamma_2(\mathbf{y})\frac{\partial \ln|\mathbf{x}-\mathbf{y}|}{\partial \mathbf{n}(\mathbf{y})}ds(\mathbf{y}) \\
&= \left(\frac{k_{eo_1}}{k_{h_1}k_{e_1}-k_{eo_1}^2}-\frac{k_{eo_2}}{k_{h_2}k_{e_2}-k_{eo_2}^2}\right)J\ln|\mathbf{x}|^2-\left(\frac{k_{h_1}}{k_{h_1}k_{e_1}-k_{eo_1}^2}-\frac{k_{h_2}}{k_{h_2}k_{e_2}-k_{eo_2}^2}\right)I\ln|\mathbf{x}|^2.
\end{aligned}
$$

- Normal Velocity

$$
V(t) = \frac{1}{2\pi}\int_{\Gamma(t)} \gamma_{1s'} \frac{(\mathbf{x}-\mathbf{x}')^{\perp}\cdot \mathbf{n}(\mathbf{x})}{|\mathbf{x}-\mathbf{x}'|^2} ds'(\mathbf{x}') + J\frac{\mathbf{x}\cdot\mathbf{n}}{|\mathbf{x}|^2}.
$$

Interface dynamics

- use arclength and tangent angle to represent the interface, $(L(t), \theta(\alpha, t))$
- use a special tangential velocity to preserve equal arclength

$$T(\alpha, t) = T(0, t) + \int_0^{\alpha} s'_{\alpha}\kappa' V d\alpha' - \frac{\alpha}{2\pi}\int_0^{2\pi} s'_{\alpha}\kappa' V d\alpha'.$$

- use 2nd order Adams-Bashforth to compute arclegth and tangent angle by introducing an integrating factor

$$s_{\alpha t} = (T_s + \kappa V)s_{\alpha}$$
$$\theta_t = -V_s + \kappa T$$

Ref: Hou, Lowengrub, Shelley, JCP 114, 1994.

Rescaling the interface dynamics

Rescaling idea

Isolate morphological change from overall growth by mapping onto a new time and space: $(x, t) \to (\bar{x}, \bar{t})$, i.e. scale out the growth: $R(t(\bar{t})) = \bar{R}(\bar{t})$.

$$x(\tilde{\alpha}, t) = \bar{R}(\bar{t})\bar{x}(\tilde{\alpha}, \bar{t}), \quad \bar{t} = \int_0^t \frac{1}{\rho(t')} dt'.$$

- $\bar{\rho}(\bar{t}) = \rho(t(\bar{t})) > 0$
  - Speed up or slow down
  - Adaptive
- The normal velocity in the rescaled frame $\bar{V}$,

$$\bar{V}(\bar{t}) = \frac{\bar{\rho}}{\bar{R}} V(t(\bar{t})) - \frac{\bar{\mathbf{x}} \cdot \mathbf{n}}{\bar{R}} \frac{d\bar{R}}{d\bar{t}}$$

- Require $\frac{d\bar{A}}{d\bar{t}} = 0$, $\int_{\bar{\Gamma}(\bar{t})} \bar{V} d\bar{s} = 0 \to \frac{d\bar{R}}{d\bar{t}} = \frac{\pi \bar{\rho} \bar{J}}{\bar{A}(0)\bar{R}}$

Li et al. (2007)
Zhao et al. (2017)

Here, we take

$\bar{\rho}(\bar{t}) = \bar{R}^2$

Exponential growth

➢ $\bar{R}(\bar{t}) = \exp(\frac{\pi \bar{J}}{\bar{A}(0)} \bar{t})$

Boundary integral equations

- Integral equation system

$$
\begin{aligned}
&\Big(\frac{k_{e_1}}{k_{h_1}k_{e_1}-k_{eo_1}^2}+\frac{k_{e_2}}{k_{h_2}k_{e_2}-k_{eo_2}^2}\Big)\bar{\gamma}_1+\frac{1}{\pi}\Big(\frac{k_{e_1}}{k_{h_1}k_{e_1}-k_{eo_1}^2}-\frac{k_{e_2}}{k_{h_2}k_{e_2}-k_{eo_2}^2}\Big)\int_{\bar{\Gamma}(\bar{t})}\bar{\gamma}_1(\bar{\mathbf{y}})\frac{\partial \ln|\bar{\mathbf{x}}-\bar{\mathbf{y}}|}{\partial \mathbf{n}(\bar{\mathbf{y}})}d\bar{s}(\bar{\mathbf{y}})\\
&-\Big(\frac{k_{eo_1}}{k_{h_1}k_{e_1}-k_{eo_1}^2}+\frac{k_{eo_2}}{k_{h_2}k_{e_2}-k_{eo_2}^2}\Big)\bar{\gamma}_2-\frac{1}{\pi}\Big(\frac{k_{eo_1}}{k_{h_1}k_{e_1}-k_{eo_1}^2}-\frac{k_{eo_2}}{k_{h_2}k_{e_2}-k_{eo_2}^2}\Big)\int_{\bar{\Gamma}(\bar{t})}\bar{\gamma}_2(\bar{\mathbf{y}})\frac{\partial \ln|\bar{\mathbf{x}}-\bar{\mathbf{y}}|}{\partial \mathbf{n}(\bar{\mathbf{y}})}d\bar{s}(\bar{\mathbf{y}})\\
&=2\tau\bar{\kappa}-\Big(\frac{k_{e_1}}{k_{h_1}k_{e_1}-k_{eo_1}^2}-\frac{k_{e_2}}{k_{h_2}k_{e_2}-k_{eo_2}^2}\Big)J\bar{R}(2\ln\bar{R}+\ln|\bar{\mathbf{x}}|^2)+\Big(\frac{k_{eo_1}}{k_{h_1}k_{e_1}-k_{eo_1}^2}-\frac{k_{eo_2}}{k_{h_2}k_{e_2}-k_{eo_2}^2}\Big)I\bar{R}(2\ln\bar{R}+\ln|\bar{\mathbf{x}}|^2),
\end{aligned}
$$

$$
\begin{aligned}
&-\Big(\frac{k_{eo_1}}{k_{h_1}k_{e_1}-k_{eo_1}^2}+\frac{k_{eo_2}}{k_{h_2}k_{e_2}-k_{eo_2}^2}\Big)\bar{\gamma}_1-\frac{1}{\pi}\Big(\frac{k_{eo_1}}{k_{h_1}k_{eo_1}-k_{eo_1}^2}-\frac{k_{e_2}}{k_{h_2}k_{e_2}-k_{eo_2}^2}\Big)\int_{\bar{\Gamma}(\bar{t})}\bar{\gamma}_1(\bar{\mathbf{y}})\frac{\partial \ln|\bar{\mathbf{x}}-\bar{\mathbf{y}}|}{\partial \mathbf{n}(\bar{\mathbf{y}})}d\bar{s}(\bar{\mathbf{y}})\\
&+\Big(\frac{k_{h_1}}{k_{h_1}k_{e_1}-k_{eo_1}^2}+\frac{k_{h_2}}{k_{h_2}k_{e_2}-k_{eo_2}^2}\Big)\bar{\gamma}_2+\frac{1}{\pi}\Big(\frac{k_{h_1}}{k_{h_1}k_{e_1}-k_{eo_1}^2}-\frac{k_{h_2}}{k_{h_2}k_{e_2}-k_{eo_2}^2}\Big)\int_{\bar{\Gamma}(\bar{t})}\bar{\gamma}_2(\bar{\mathbf{y}})\frac{\partial \ln|\bar{\mathbf{x}}-\bar{\mathbf{y}}|}{\partial \mathbf{n}(\bar{\mathbf{y}})}d\bar{s}(\bar{\mathbf{y}})\\
&=\Big(\frac{k_{eo_1}}{k_{h_1}k_{e_1}-k_{eo_1}^2}-\frac{k_{eo_2}}{k_{h_2}k_{e_2}-k_{eo_2}^2}\Big)J\bar{R}(2\ln\bar{R}+\ln|\bar{\mathbf{x}}|^2)-\Big(\frac{k_{h_1}}{k_{h_1}k_{e_1}-k_{eo_1}^2}-\frac{k_{h_2}}{k_{h_2}k_{e_2}-k_{eo_2}^2}\Big)I\bar{R}(2\ln\bar{R}+\ln|\bar{\mathbf{x}}|^2).
\end{aligned}
$$

- Normal velocity

$$
\bar{V}(\bar{\mathbf{x}})=\frac{1}{2\pi\bar{R}}\int_{\bar{\Gamma}(\bar{t})}\bar{\gamma}_{1\bar{s}}\frac{(\bar{\mathbf{x}}'-\bar{\mathbf{x}})^{\perp}\cdot\bar{\mathbf{n}}(\bar{\mathbf{x}})}{|\bar{\mathbf{x}}'-\bar{\mathbf{x}}|^2}d\bar{s}'+\bar{J}\frac{\bar{\mathbf{x}}\cdot\bar{\mathbf{n}}}{|\bar{\mathbf{x}}|^2}-\frac{\pi\bar{J}}{\bar{A}(0)}\bar{\mathbf{x}}\cdot\bar{\mathbf{n}},
$$

- Interface dynamics

$$
\frac{d\bar{\mathbf{x}}(\bar{t},\theta)}{d\bar{t}}\cdot\mathbf{n}=\bar{V}(\bar{t},\theta).
$$

Numerical method

- Pseudo-spectral method on interface
- Spectrally accurate spatial discretization (alternating point trapezoidal rule)
- 2nd order Adams-Bashforth in time
- Small scale decomposition to remove numerical stiffness (Hou, L., Shelley, 1994)

Parameters from Gao et al. (2019)

$k_{h_1} = 14.93$, $k_{h_2} = 1$, $k_{eo_1} = 0$, $k_{eo_2} = 1.93 \times 10^{-4}$, and $k_{e_1} = k_{e_2} = 2.66$. $\tau = 0.0216$

Convergence study

- $\tau = 2.16 \times 10^{-2}$, $r(\tilde{\alpha}, 0) = 1 + 0.1\cos(4\tilde{\alpha})$, $J = 1$, and $I = -636$.
- Temporal study: $N = 4096$, $\Delta\bar{t} = 2 \times 10^{-3}$, 1×10^{-3}, and 5×10^{-4}.
- Spatial study: $\Delta\bar{t} = 1 \times 10^{-4}$, $N = 1024$, 2048, and 4096.
- Error: $Error = |\bar{A}_{\bar{t}} - \bar{A}_0|$.

2[nd] order accurate in time

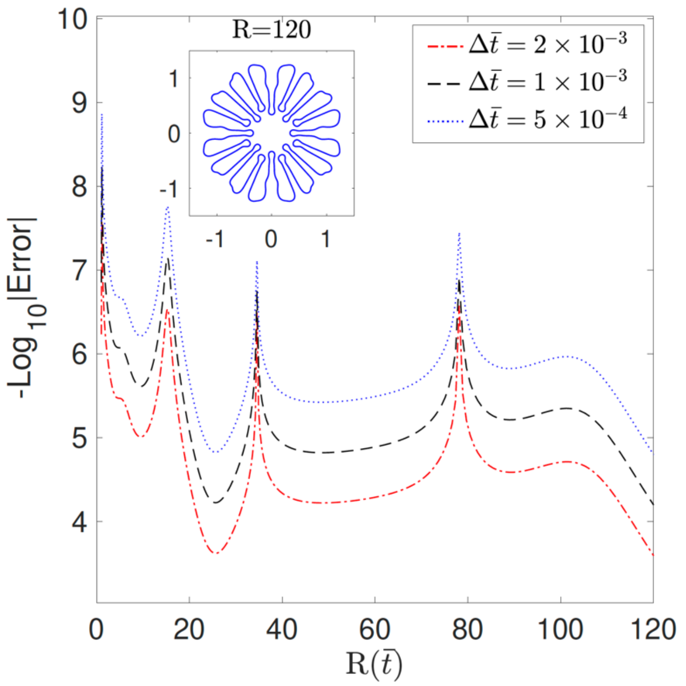

(a)

Spectrally accurate in space

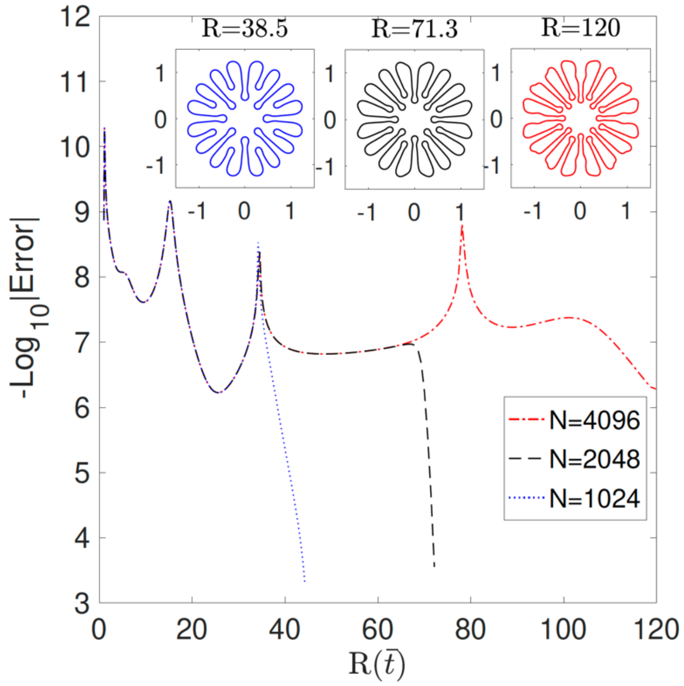

(b)

Agreement with linear theory at small perturbations

- $\tau = 2.16 \times 10^{-2}$, $\Delta\bar{t} = 1 \times 10^{-3}$, $N = 4096$, $r(\tilde{\alpha}, 0) = 1 + 0.05\cos(4\tilde{\alpha})$, $J = 1$, and $I = -636$.
- Linear solution:

$$(\frac{\delta}{R})_{Lin} = (\frac{\delta}{R})_0 R^{\frac{(k_{eo_2} k_{h_1} - k_{eo_1} k_{h_2})}{(k_{eo_1} + k_{eo_2})^2 - (k_{e_1} + k_{e_2})(k_{h_1} + k_{h_2})} \frac{2nI}{J} + (n \frac{k_{eo_1}^2 - k_{eo_2}^2 - (k_{e_1} + k_{e_2})(k_{h_1} - k_{h_2})}{(k_{eo_1} + k_{eo_2})^2 - (k_{e_1} + k_{e_2})(k_{h_1} + k_{h_2})} - 2)}$$

$$\exp\left[\frac{(k_{eo_2}^2 k_{h_1} + (k_{eo_1}^2 - (k_{e_1} + k_{e_2}) k_{h_1}) k_{h_2})}{(k_{eo_1} + k_{eo_2})^2 - (k_{e_1} + k_{e_2})(k_{h_1} + k_{h_2})} \frac{n(n^2 - 1)\tau}{J} (R^{-1} - 1)\right].$$

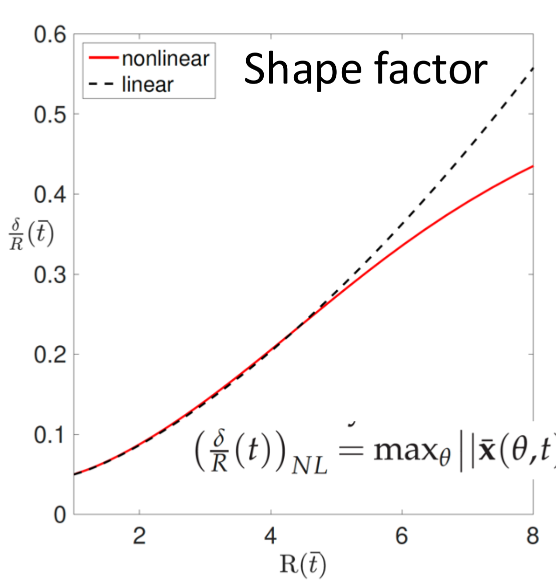

(a)

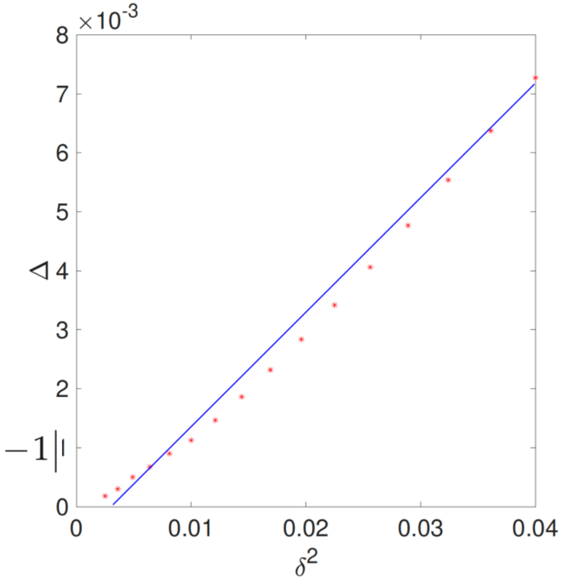

(b)

Deviation between linear and nonlinear results is 2nd order in perturbation size

Effect of electro-osmotic flow

- $\tau = 2.16 \times 10^{-2}$, $\Delta \bar{t} = 1 \times 10^{-3}$, $N = 4096$, $r(\tilde{\alpha}, 0) = 1 + 0.1\cos(4\tilde{\alpha})$, and $J = 1$.
- $I = 28I_0$ (black), $I = 0$ (red), $I = -28I_0$ (blue), $I_0 = -159$,.

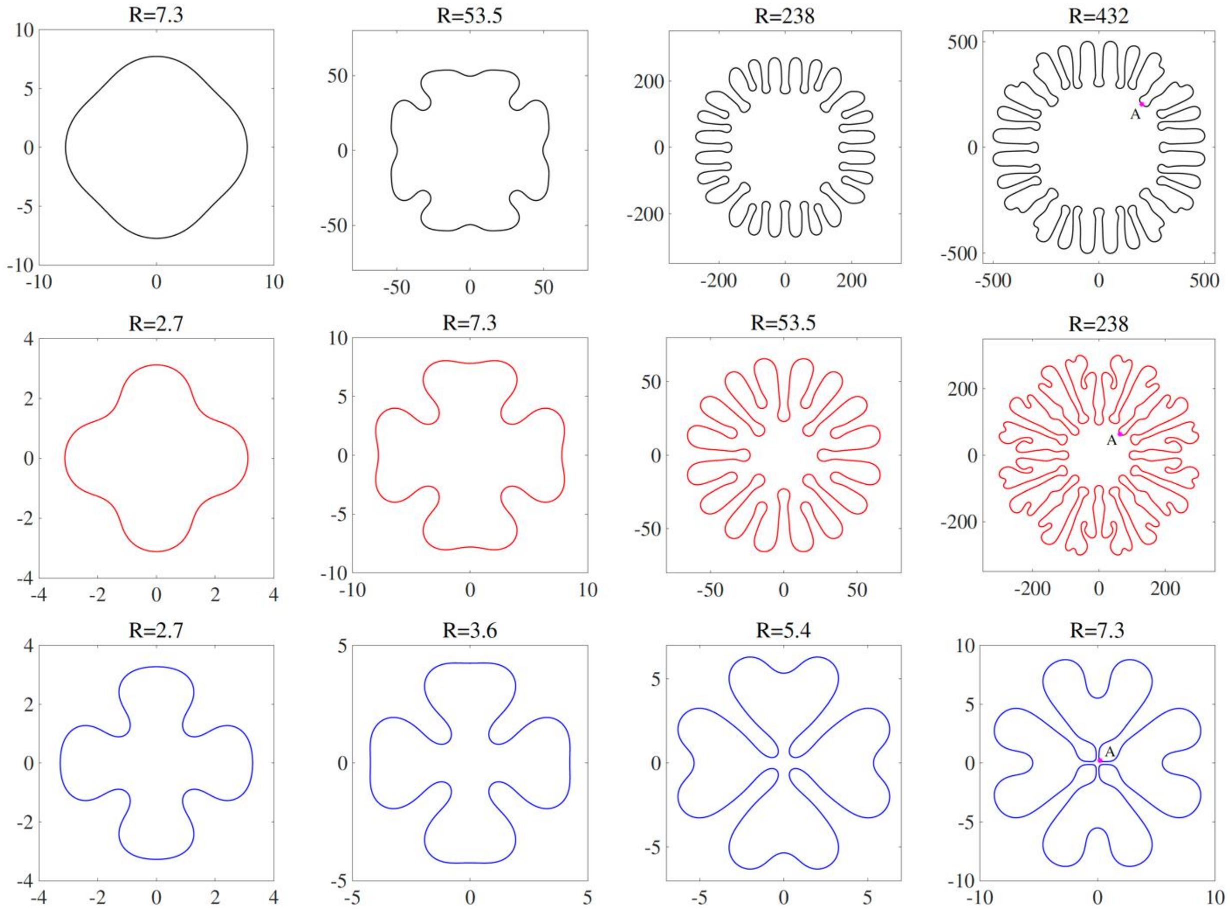

Stabilizing electric current

No electric current

Destabilizing electric current

Effect of electro-osmotic flow II

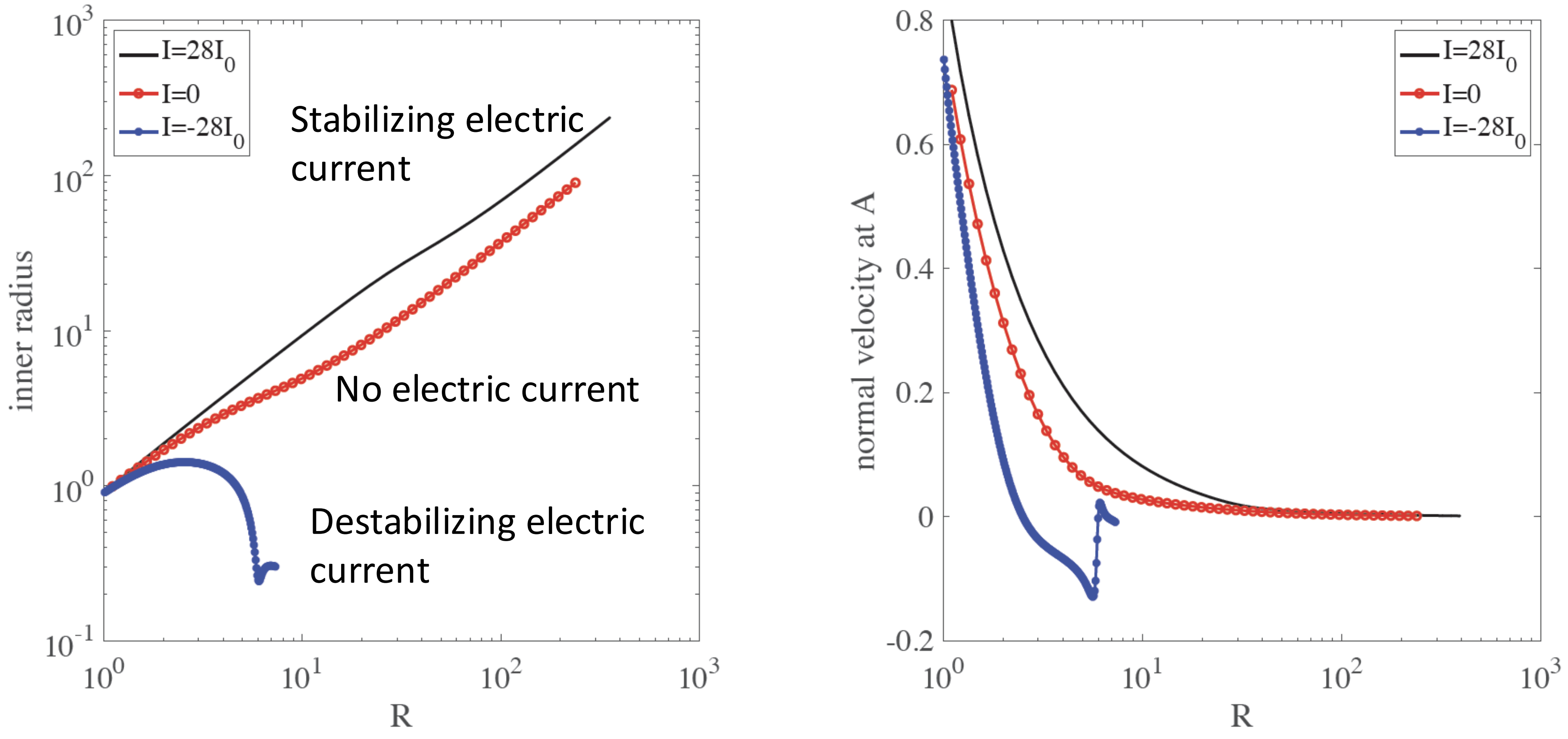

Effect of surface tension

- $\tau = 5 \times 10^{-4}$, $\Delta\bar{t} = 1 \times 10^{-3}$, $N = 4096$, $r(\tilde{\alpha}, 0) = 1 + 0.1\cos(4\tilde{\alpha})$.
- $J = 1$, and $I = -28I_0$, $I_0 = -159$.

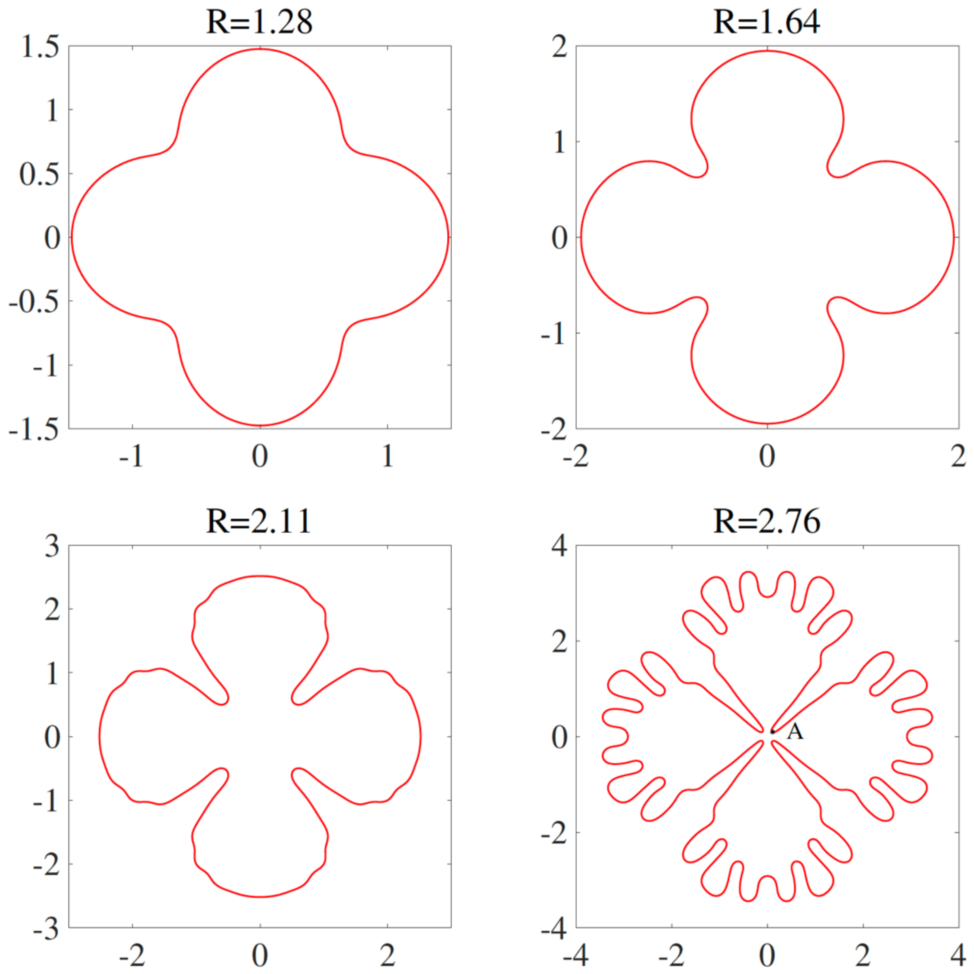

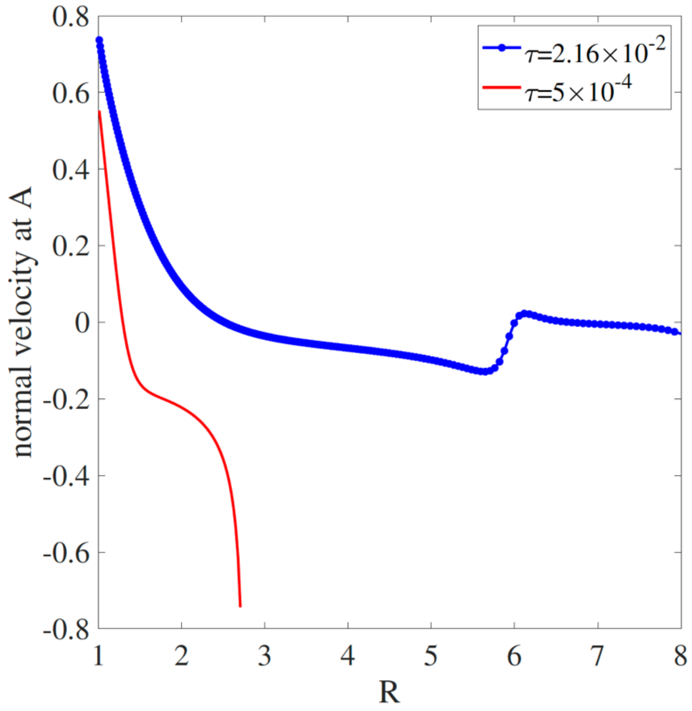

Electro-osmotic flow (no injection flux)

- $\tau = 2.16 \times 10^{-2}$, $\Delta\bar{t} = 1 \times 10^{-3}$, $N = 4096$, $r(\tilde{\alpha}, 0) = 1 + 0.1\cos(n\tilde{\alpha})$.
- $J = 0$ and $I = -150I_0$, $I_0 = -159$.

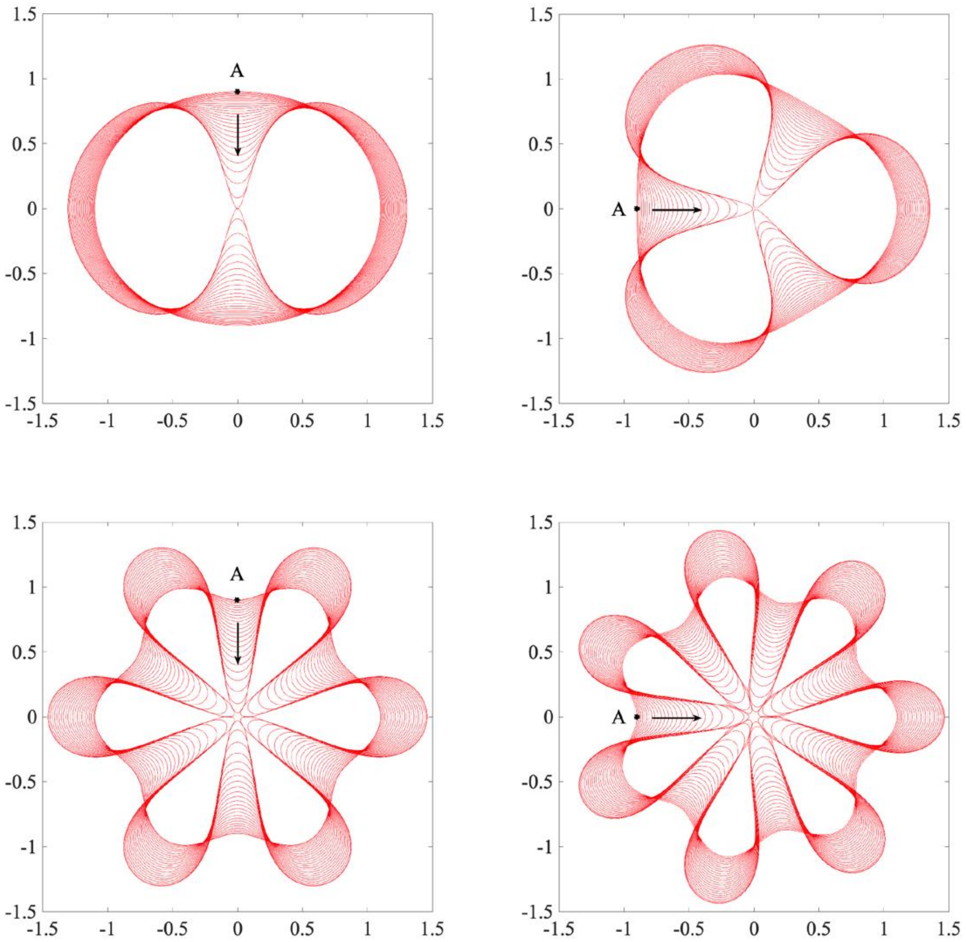

- Destabilizing electro-osmotic field drives pinchoff and finite time singularities.

Electro-osmotic flow (no injection flux)

- Inner radius fits an algebraic law $(t_* - t)^b$, where t_* is the estimated time when the interface reaches the origin.
- $n = 2$, $t_* = 0.520$ and $b = 0.570$.
- $n = 7$, $t_* = 0.478$ and $b = 0.615$.

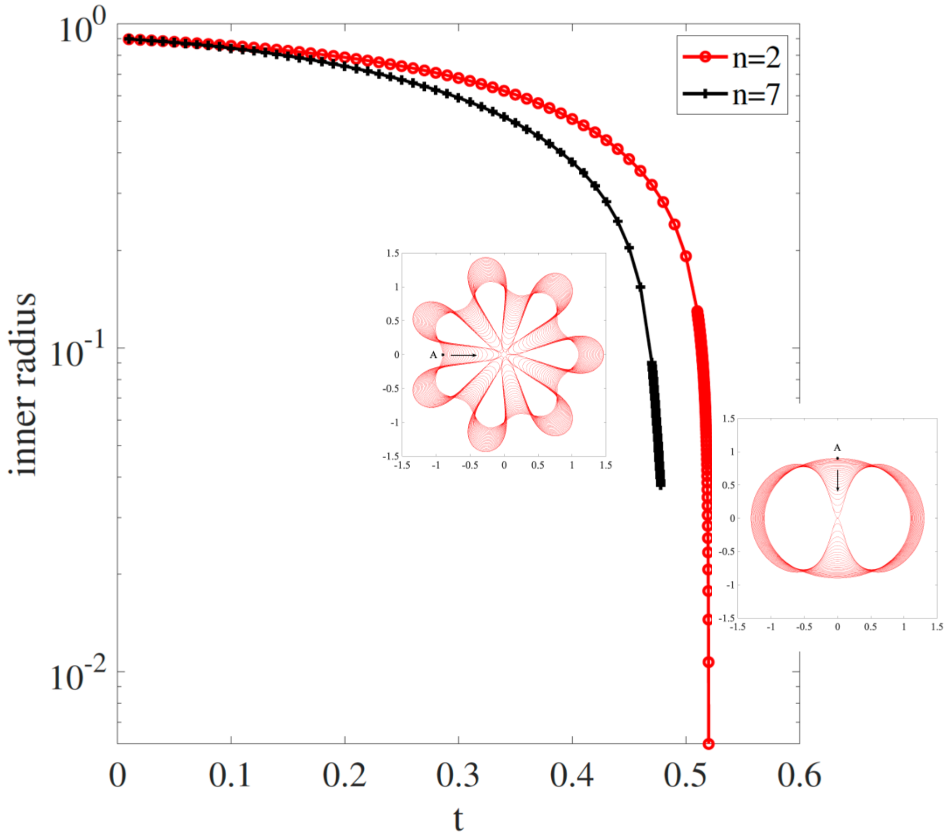

Effects of electric current and surface tension

- $r(\tilde{\alpha}, 0) = 1 + 0.1\cos(2\tilde{\alpha})$, $\tau = 2.16 \times 10^{-2}$, different I.
- $r(\tilde{\alpha}, 0) = 1 + 0.1\cos(2\tilde{\alpha})$, $I = -150 I_0$, different τ.

Destabilizing current

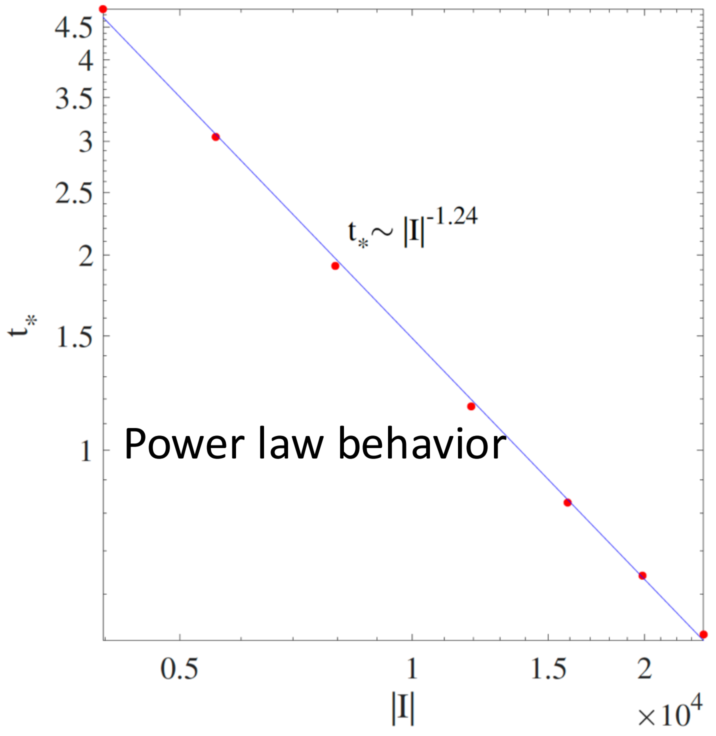

(a)

Stabilizing surface tension

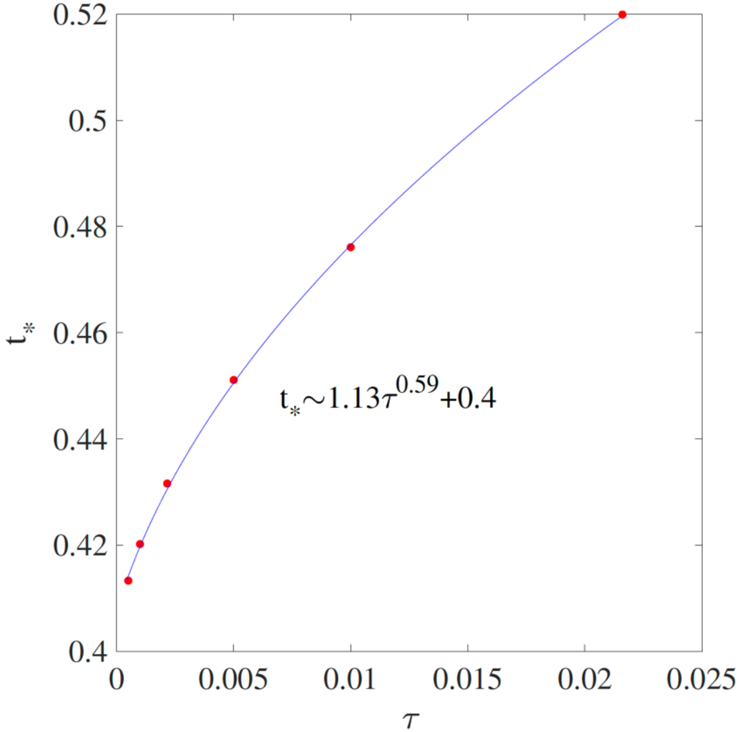

(b)

Can we actually specify the shapes?

Self-similar limiting dynamics

- $r(\tilde{\alpha}, 0) = 1 + 0.01(\sin(2\tilde{\alpha}) + \cos(3\tilde{\alpha}) + \sin(5\tilde{\alpha}) + \cos(7\tilde{\alpha}))$.
- $J = \alpha J_{crit}(n_{max}),\ n_{max} = 7,$

$$J_{crit} = \frac{n_{max}^3 \tau}{R} \frac{[k_{eo_2}^2 k_{h_1} + (k_{eo_1}^2 - (k_{e_1} + k_{e_2})k_{h_1})k_{h_2}]}{(k_{eo_1} + k_{eo_2})^2 - (k_{e_1} + k_{e_2})(k_{h_1} + k_{h_2})},$$

$$I_c = \Big(- [k_{eo_1}^2 - k_{eo_2}^2 - (k_{e_1} + k_{e_2})(k_{h_1} - k_{h_2})]J + \frac{\tau \mathcal{C}}{R}[k_{eo_2}^2 k_{h_1} + (k_{eo_1}^2 - (k_{e_1} + k_{e_2})k_{h_1})k_{h_2}] \Big) / 2(k_{eo_2} k_{h_1} - k_{eo_1} k_{h_2}).$$

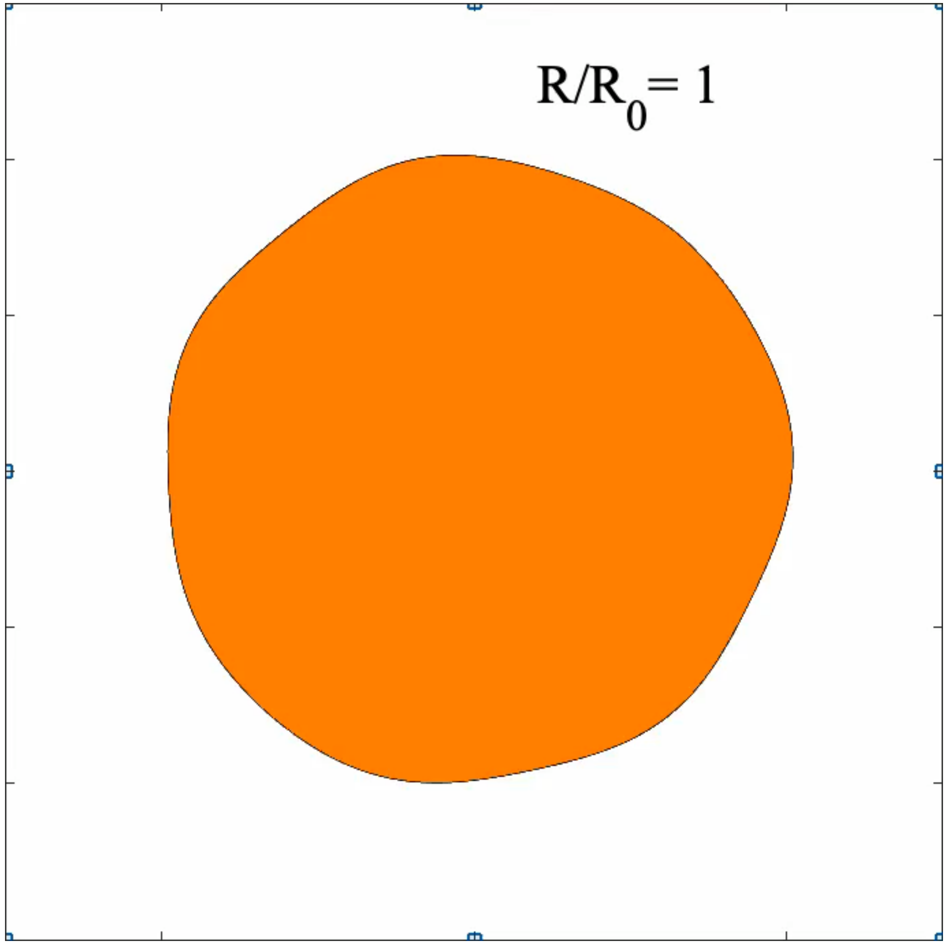

Self-similar limiting dynamics

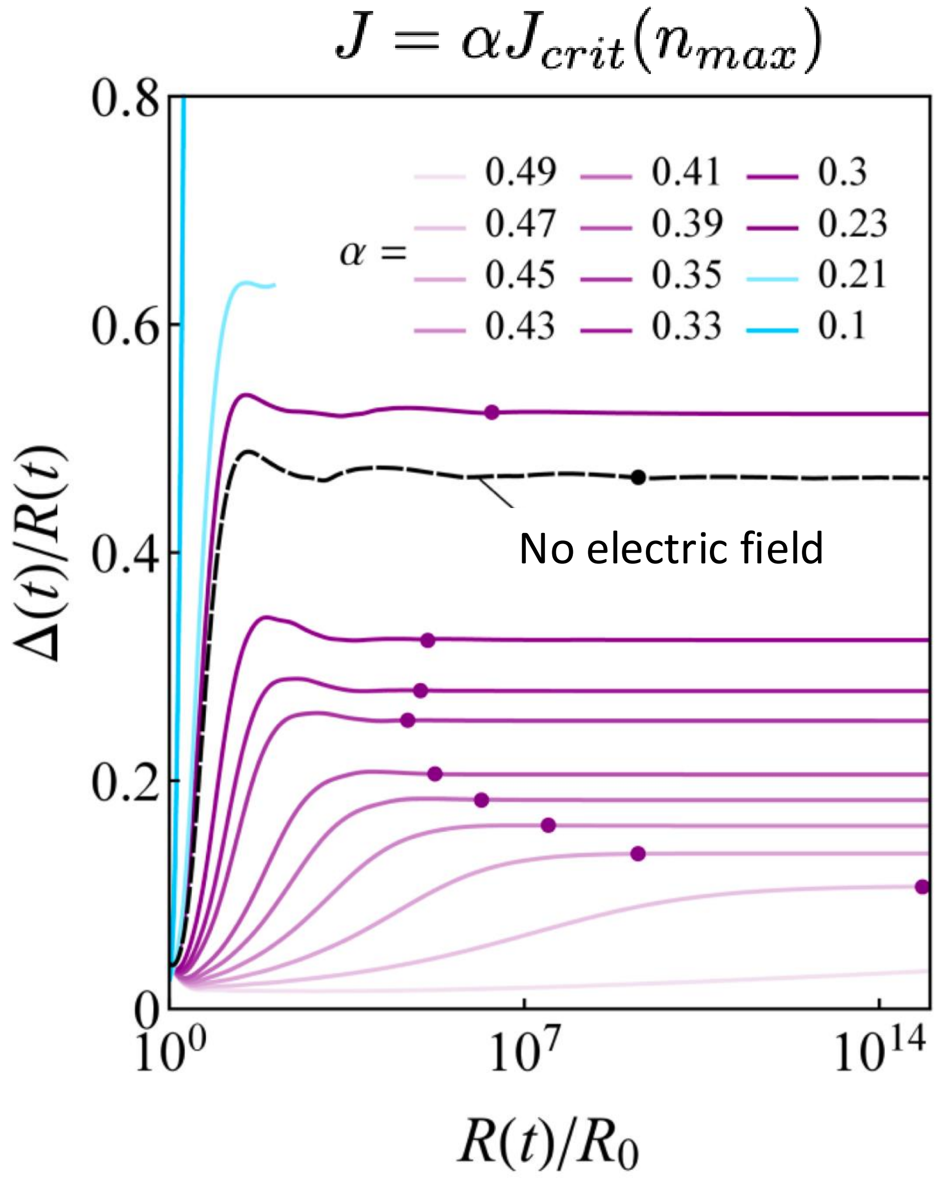

α Controls

- Magnitude of perturbation (α decreases, shape is more perturbed)
- Time at which evolution becomes self-self similar (non-monotone function of α)

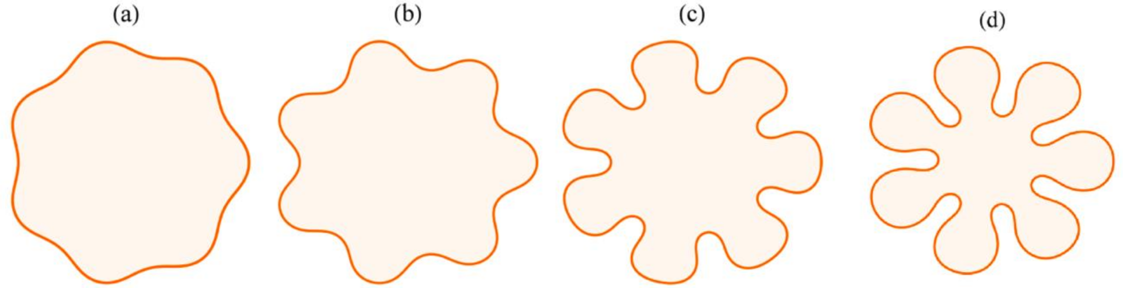

$\alpha = 0.49$	$\alpha = 0.45$	$\alpha = 0.3$	$\alpha = 0.23$
$R/R_0 = 10^{36}$	$R/R_0 = 10^9$	$R/R_0 = 10^5$	$R/R_0 = 10^6$

Behavior at smaller α: Pinch-off

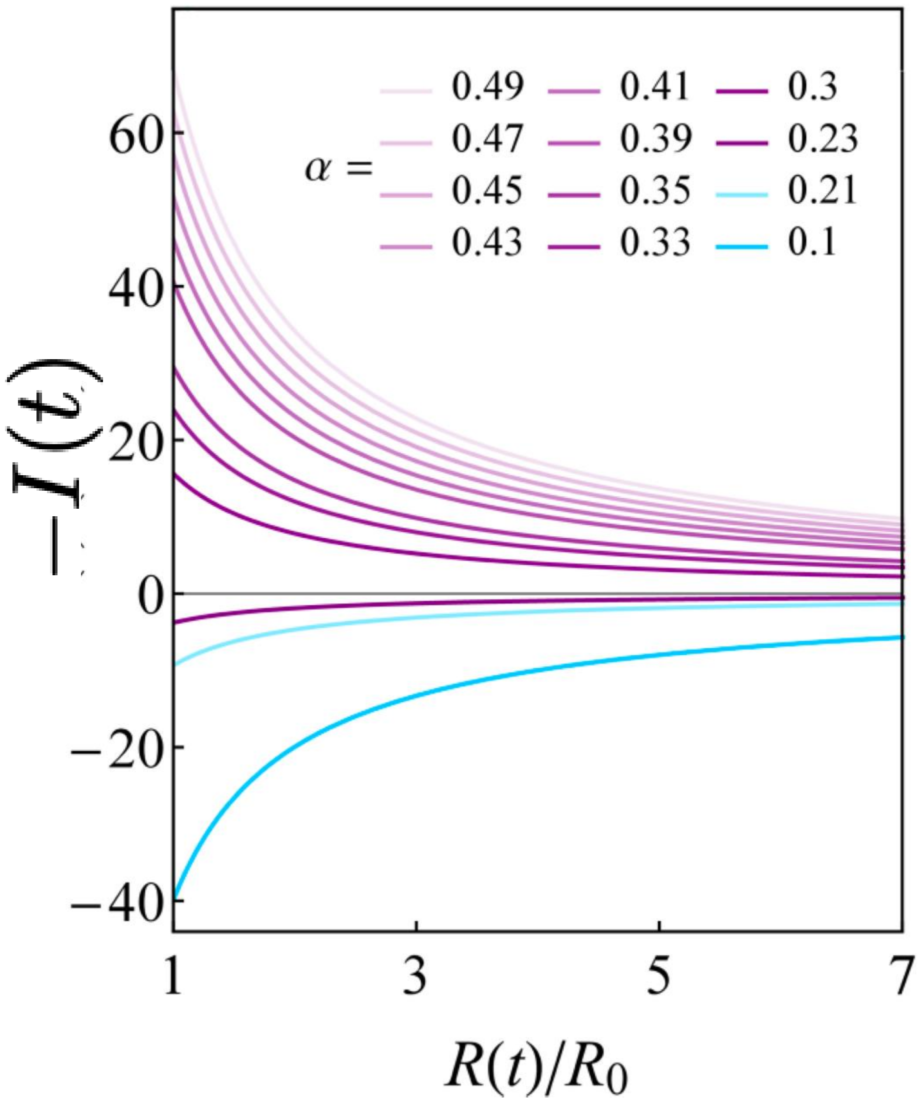

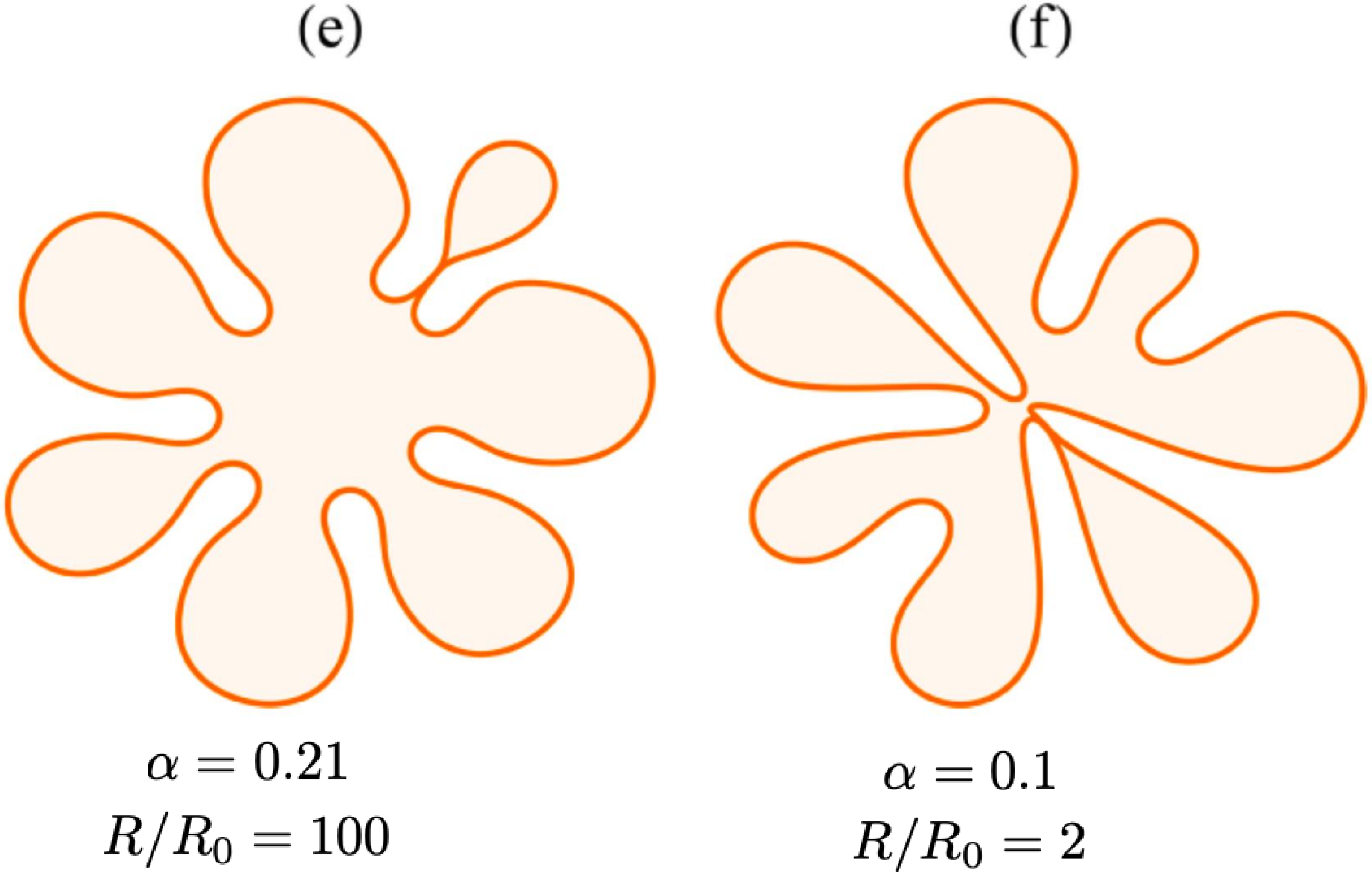

- I(t) becomes sufficiently positive

Other modes I

$$n_{max} = 3$$

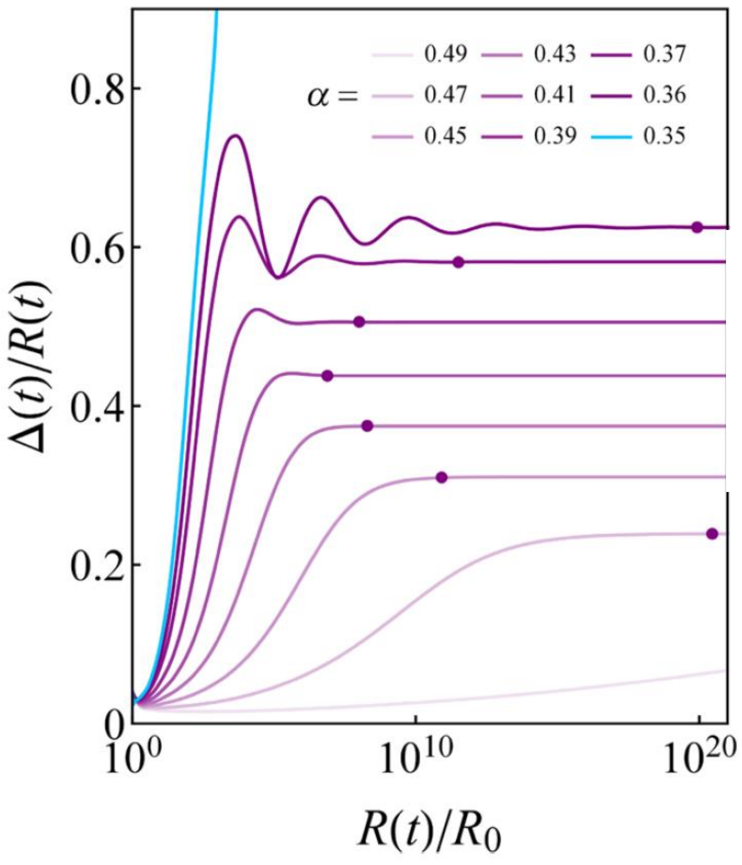

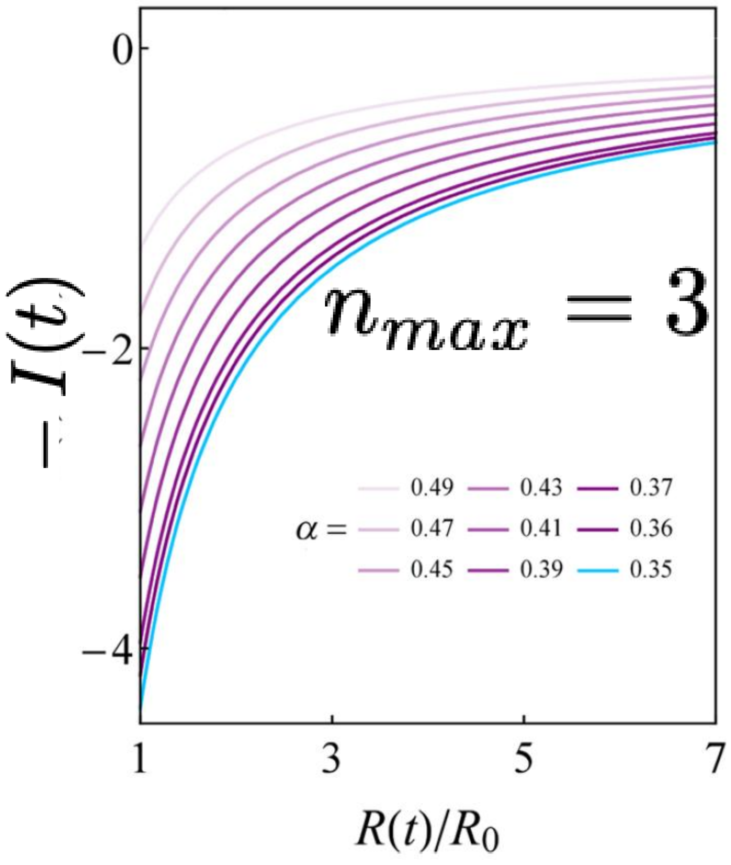

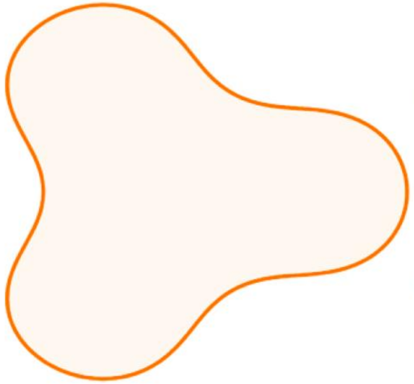

$\alpha = 0.45$

$R/R_0 = 10^{11}$

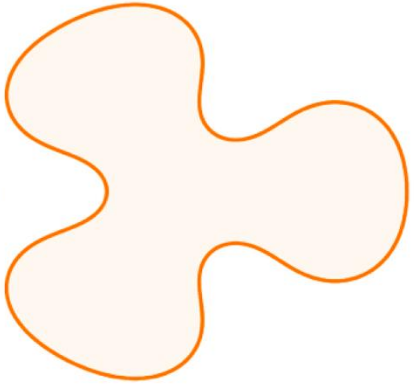

$\alpha = 0.37$

$R/R_0 = 10^{11}$

Does not reach equilibrium.

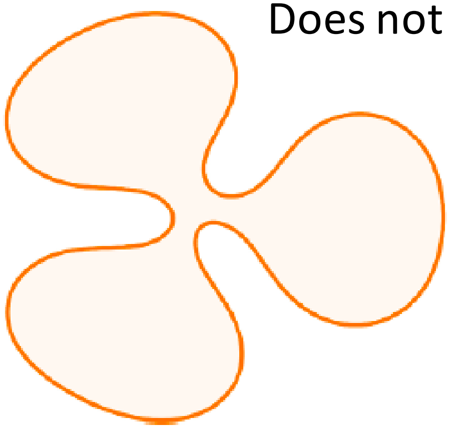

$\alpha = 0.35$

$R/R_0 = 10^3$

Other modes II

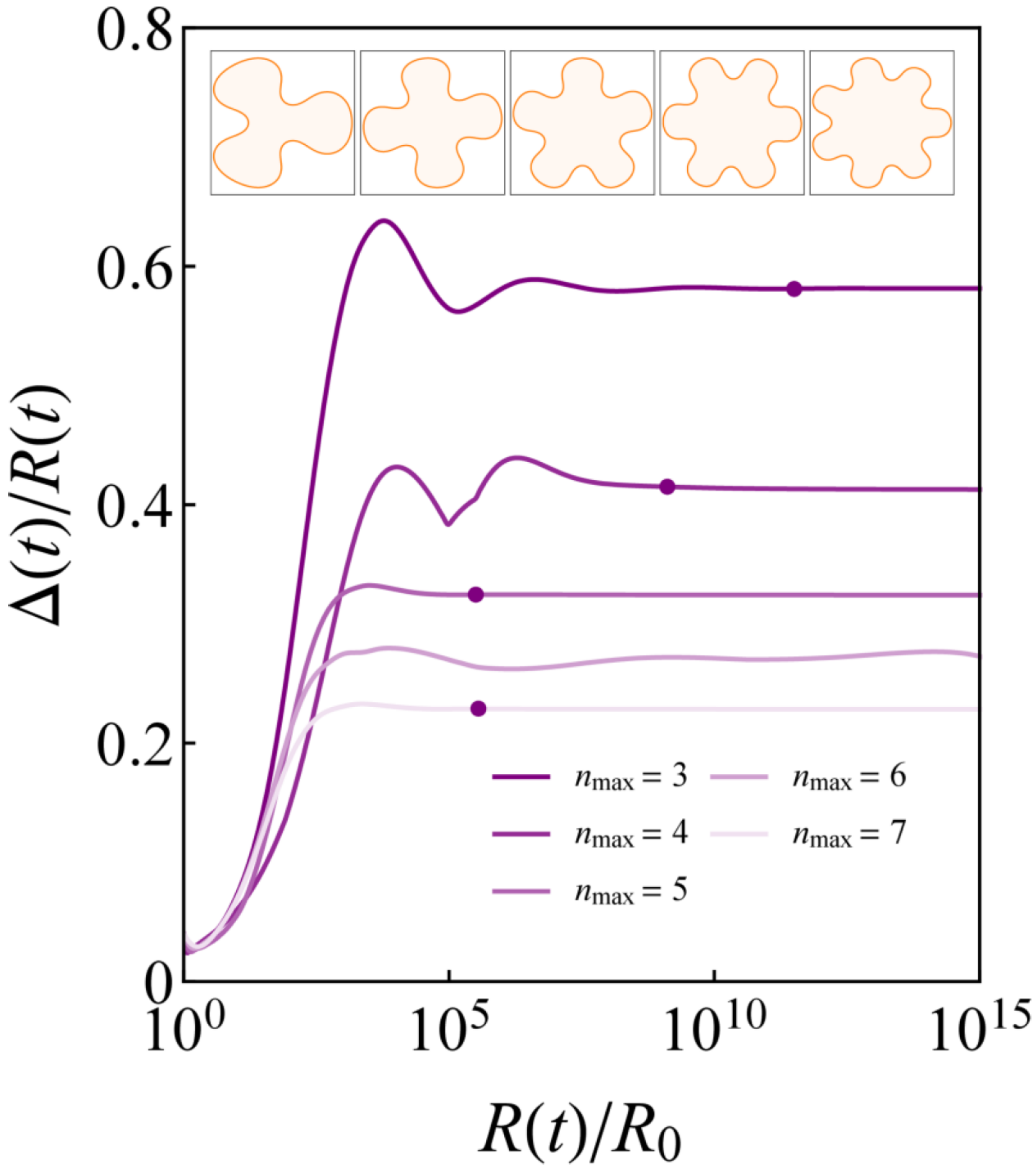

$\alpha = 0.37$

Behavior is qualitatively similar

Conclusions and Future work

- Investigated interfacial instabilities in a Hele-Shaw cell under an electric field
- Developed efficient, accurate numerical method
- Electro-osmotic flow can enhance or decrease morphological instabilities
- Possible to control shape (self-similar evolution). Mode selection. Additional parameter compared to case without electric field. Can control size and time of onset.
- Randomness. Multimodal initial condition gives fastest evolution to limiting shape.
- Future. Consider other fluxes. Multi-field driven interfaces. (e.g., magnetic fields, etc.)